Automatica 182 (2025) 112526

Contents lists available at ScienceDirect

Automatica

journal homepage: www.elsevier.com/locate/automatica

Observer-based detection and isolation of permanent sensor faults in a class of uncertain switched affine systems ☆

Diego dos Santos Carneiro [a,*], Flávio Andrade Faria [b], Vilma Alves de Oliveira [a], Michele Cucuzzella [d], Antonella Ferrara [c]

[a] Department of Electrical and Computer Engineering, Universidade de São Paulo (USP), Sao Carlos, Brazil
[b] Department of Mathematics, School of Engineering, Sao Paulo State University (UNESP), Ilha Solteira, Brazil
[c] Department of Electrical, Computer and Biomedical Engineering, The University of Pavia (UNIPV), Pavia, Italy
[d] Engineering and Technology Institute Groningen, The University of Groningen, Groningen, Netherlands

ARTICLE INFO

Article history:
Received 13 May 2024
Received in revised form 16 May 2025
Accepted 24 June 2025
Available online 23 August 2025

Keywords:
Fault detection and isolation
Switched systems
Uncertain systems

ABSTRACT

This paper develops a robust fault detection and isolation (FDI) strategy for a class of uncertain continuous-time switched affine systems when the system state is not fully available for measurement, and all system sensors are prone to permanent abrupt bounded faults. The FDI strategy is obtained by designing a number of FDI devices equal to the number of sensors. First, we give linear matrix inequalities conditions to design a bank of full-state Luenberger observers in a pseudo-dedicated scheme with guaranteed $\mathcal{S}_-$ and $\mathcal{L}_\infty$ performances to work as residual error generators (REGs). In the sequence, considering an extension of the concepts of weak and strong detectability and novel concepts of weak and strong isolation, residual evaluation functions are defined, and threshold functions are designed considering the gains and parameters obtained in the REG design, taking into consideration the smallest fault magnitude to be detected to achieve a mixed $\mathcal{S}_-/\mathcal{L}_\infty$ performance. An Algorithm to determine a piecewise constant threshold function is proposed to obtain less conservative constraints in the optimization problem. Furthermore, parameter-tuning algorithms are proposed to obtain local optima thresholds and REGs to satisfy weak isolation conditions over a range of uncertainties. Finally, a Cuk DC–DC converter is considered to demonstrate the effectiveness of the proposed approach.

1. Introduction

Observer-based strategies working as residual error generators for mitigating disturbances and detecting faults in dynamic systems have gained prominence in the literature. Recent advancements in isolating, reconstructing, and mitigating the effects of disturbances, as well as addressing a class of communication attacks have appeared (Rinaldi, Menon, Edwards, Ferrara, & Shtessel, 2021). In the context of switched systems switched, Marouani, Nguyen, Dinh, and Raïssi (2024) and Hao and Huang (2024) propose observers to detect faults in discrete-time switched systems and Ali et al. (2024) designs observers with a guaranteed $\mathcal{H}_\infty/\mathcal{H}_-$ attenuation /sensitivity performance for a class of continuous-time switched systems under sensor faults and disturbances. In Rinaldi, Cucuzzella, Menon, Ferrara, and Edwards (2022), the authors propose an observer-based approach to detect load-altering attacks in switched systems that may cause critical faults, while Ribeiro, Carneiro, Costa, and Oliveira (2022) considers switched Markovian jump systems in the design of the residual error generators to detect covert attacks in cyber–physical systems. Fault detection and isolation (FDI) strategies for a class of continuous-time switched affine systems strategies for switched affine systems are proposed in Li, Ma, and Zhao (2021) and Carneiro, Silva, Faria, Magossi, and Oliveira (2021). Although, fault-tolerance switching laws for uncertain continuous-time switched affine systems (SAS) subject to additive sensor faults have been considered in the literature (Carneiro, Faria, Silva, Zilli, & Oliveira, 2024), the problem of FDI of multiple permanent faults in uncertain SAS using an observer-based approach with sensitivity and attenuation performances under permanent faults and uncertainties is not extensively discussed in the literature.

Usually, to guarantee the detection and isolation of multiple sensor or actuator faults in a system, a bank of observer-based residual error generators can be designed in a generalized observer scheme (GOS) or dedicated observer scheme (DOS) (Blanke, Kinnaert, Lunze, & Staroswiecki, 2016; Commault,

☆ The material in this paper was not presented at any conference. This paper was recommended for publication in revised form by Associate Editor Angelo Alessandri under the direction of Editor Thomas Parisini.

* Corresponding author.
E-mail addresses: diegocarneiro@usp.br (D. dos Santos Carneiro), flavio.faria@unesp.br (F.A. Faria), voliveira@usp.br (V.A. de Oliveira), m.cucuzzella@ieee.org (M. Cucuzzella), antonella.ferrara@unipv.it (A. Ferrara).

https://doi.org/10.1016/j.automatica.2025.112526
0005-1098/

Dion, Sename, & Motyeian, 2002), such that it is possible to determine which component is faulty without the need to estimate the fault magnitude. The recent work Sacchi, Incremona, and Ferrara (2023), proposes an active FDI structure to detect and isolate multiple faults by using a mixed model-based and data-driven strategy using a bank of observers, but the authors consider an estimation of the fault magnitude, which can be challenging to obtain for uncertain SAS. On the other hand, to determine only the location of the fault,i.e., which component is faulty, the classical DOS guarantees better fault isolation at the cost of observability reduction and less robustness, whereas GOS improves the observability and robustness properties (Capisani, Ferrara, De Loza, & Fridman, 2012), but multiple faults cannot be detected. Thus, a mixed structure using the philosophy of dedicated fault detection with a dedicated observer scheme by preserving observability, as in the GOS, is an alternative when all sensors are prone to faults, and multiple faults should be detected.

However, to achieve fault isolation, the observers must be sensitive to a specific set of sensor faults and robust against uncertainties and faults that do not belong to the set of faults to be detected (Blanke et al., 2016). An alternative to guarantee attenuation and sensitivity performance is by designing the gains of the observers considering a mixed $\mathcal{H}_-/\mathcal{H}_\infty$ performance, as in Ali et al. (2024), Du, Yang, Zhao, and Tan (2020), Hao and Huang (2024), Su, Fan, and Li (2019). However, $\mathcal{H}_\infty$-based strategies are not suitable to the design fault detection observers with a given attenuation performance for certain classes of bounded faults, particularly permanent faults, which are faults that can last for long periods since their magnitude does not trigger any protective device (Greber, Fodor, & Magyar, 2020). Specifically, when the magnitude of the fault remains greater than zero for all time after the fault occurrence, performances such as the $\mathcal{H}_\infty$-based cannot be applied, and $\mathcal{L}_\infty$-based performances as in Li et al. (2021), Xie, Zong, Yang, Chen, and Shi (2022) need to be considered. Moreover, to the best of our knowledge, a comprehensive sensitivity performance for permanent sensor faults in uncertain SAS has not been reported in the literature, although Reppa, Timotheou, Polycarpou, and Panayiotou (2017) proposes an optimization method to obtain the gains of the observers to enhance sensitivity to permanent faults.

Also, concepts such as weak or strong detectability can be considered as a property of the residual generator with respect to permanent faults, as in Blanke et al. (2016), Reppa, Polycarpou, and Panayiotou (2016), Reppa et al. (2017), and the observer design can take these concepts into consideration. In addition, weak and strong isolation concepts are introduced in Gertler and McAvoy (1997), but this topic is not widely explored in the FDI literature. Furthermore, with the assumption that all sensors are prone to faults and the system is subject to uncertainties, it is challenging to provide full fault isolation since the residual error generator can be affected by uncertainties and by faults that are not supposed to be detected, referred to as remaining faults, which highlights the importance of the establishment of residual evaluation functions as in Reppa, Timotheou, Polycarpou, and Panayiotou (2018), such that a fault is detected whenever the magnitude of this function is greater than a given threshold. Moreover, the selection of thresholds must account for the effects of uncertainties and residual faults to prevent false alarms (Alwi, Edwards, & Tan, 2011), and a method to obtain the threshold values for uncertain SAS has not yet been addressed.

This paper addresses the critical issue of fault detection and isolation for a class of continuous-time uncertain SAS when all sensors are subject to additive permanent faults, and the system state is not fully available for measurements. The strategy proposed in this paper is applied for situations where the classical dedicated observer and generalized schemes cannot be applied to detect and isolate faults in multiple sensors, where multiple faults, which may be simultaneous, are detected by using a strategy to infer that if two or more residuals are affected, then faults occur in different sensors. The main contributions of this paper are summarized as follows:

1. Differing from the classical and generalized dedicated observer schemes, we consider a pseudo-dedicated observer scheme for the FDI strategy with a bank of full-order observers working as residual error generators, where the observer of index ℓ is designed to detect faults in the sensor of the same index, whereas the effect of system uncertainties and faults in other sensors are attenuated in the residual error generator.
2. We guarantee $\mathcal{S}_-$ and $\mathcal{L}_\infty$ performances in the observer's design, improving robustness and observability properties in relation to the classical dedicated observer scheme, and the stability of each residual error generator is analyzed in terms of linear matrix inequalities (LMIs).
3. We extend the definition of strong and weak detection given in Reppa et al. (2018) by including a desired fault magnitude to be detected and a range of uncertainties in which weak or strong isolation are guaranteed. This is achieved by considering threshold functions obtained using the solution of LMI-based optimization problems, ensuring a mixed $\mathcal{S}_-/\mathcal{L}_\infty$ sensitivity/attenuation performance.
4. We provide a tuning algorithm to improve the sensitivity/attenuation performance of all residual error generators.

The remaining of the paper is organized as follows. Section 2 presents the mathematical background for the main results, and Section 3 presents the problem formulation. Section 4 presents the main results on the design of FDI devices. Section 5 shows numerical results obtained by applying the proposed strategy for the detection and isolation of sensor faults in a DC–DC Cuk Converter. Finally, Section 6 presents the conclusion and future directions of the current work.

Notations

The symbol $\star$ denotes the transposed element in symmetric matrices, $(')$ indicates transpose and $\dagger$ denotes the right pseudo-inverse. For symmetric matrices, $\mathbf{M} \prec \mathbf{0}$ ($\mathbf{M} \succ \mathbf{0}$) indicates that $\mathbf{M}$ is negative (positive) definite and $\mathbf{M} \preceq \mathbf{0}$ ($\mathbf{M} \succeq \mathbf{0}$) indicates that $\mathbf{M}$ is negative (positive) semi-definite. The operator $\text{He}(\mathbf{M})$ denotes the following sum of matrices: $\text{He}(\mathbf{M}) := \left(\mathbf{M} + \mathbf{M}'\right)$. The maximum and minimum eigenvalue of a square real matrix $\mathbf{M}$ is denoted as $\lambda_{\max}(\mathbf{M})$ and $\lambda_{\min}(\mathbf{M})$, respectively. For $\mathbf{A}$ and $\mathbf{B}$ positive definite matrices, $\mathbf{A} \succeq \mathbf{B}$ implies that $\mathbf{A} - \mathbf{B} \succeq \mathbf{0}$. The set composed by the first $\mathscr{M}$ positive integers is denoted by $\mathbb{I}_{\mathscr{M}} := \{1, \ldots, \mathscr{M}\}$, where $\mathscr{M}$ is a finite positive integer corresponding to the number of system modes. For a matrix in the set $\mathcal{M} = \{\mathbf{M}_1, \ldots, \mathbf{M}_i, \ldots, \mathbf{M}_{\mathscr{M}}\}$, $\overline{\lambda}_{\max}(\mathbf{M}_i) := \max_{i \in \mathbb{I}_{\mathscr{M}}}(\lambda_{\max}(\mathbf{M_i}))$ and $\underline{\lambda}_{\min}(\mathbf{M}_i) := \min_{i \in \mathbb{I}_{\mathscr{M}}} \lambda_{\min}(\mathbf{M}_i)$. The set of real non-negative numbers is denoted by $\mathbb{R}_+$. The ∞-norm of a function $f : \mathbb{R} \to \mathbb{R}$ in the Lebesque measurable space $\mathcal{L}_\infty$ is denoted by $\|f\|_{\mathcal{L}_\infty}$ where $\|f\|_{\mathcal{L}_\infty} := \sup_{\tau \in [T_0, t]} (|f(\tau)|)$ with $|f|$ the absolute value of f, and the 1-norm of f in the Lebesgue measurable space $\mathcal{L}_1$ is denoted by $\|f\|_{\mathcal{L}_1}$. The Euclidean norm of a vector $x \in \mathbb{R}^n$ is denoted by $\|x\|$. A $\mathcal{C}^1$ is function is a continuous function which is differentiable and has a continuous fist time derivative. The notation $\text{sign}(f)$ is the signum function, where $\text{sign}(f) = 1$, if $f > 0$, $\text{sign}(f) = -1$, if $f < 0$ and $\text{sign}(f) = 0$, if $f = 0$.

2. Preliminaries

The following definitions and results are required to obtain the main contributions developed in this work.

Definition 1. Let $f : \mathbb{R} \to \mathbb{R}$ and let $\eta > 0$ be a scalar. Functionals $G : \mathbb{R} \times \mathbb{R}_+ \to \mathbb{R}$ and $F : \mathbb{R} \times \mathbb{R}_+ \to \mathbb{R}$ are defined as

$$\mathbf{G}(f, t) := \int_0^t e^{-\eta(t-\tau)} f(\tau) d\tau \tag{1}$$

$$\mathbf{F}(f, T_0, t) := \int_{T_0}^t e^{-\eta(t-\tau)} f(\tau) d\tau. \tag{2}$$

Lemma 1. *Let $f := \|v\|^2$ with $v : \mathbb{R}^q \times \mathbb{R}_+ \to \mathbb{R}$, bounded and measurable on $[T_0, t]$. The equality $\|v\|^2_{\mathcal{L}_\infty} = \eta \sup_{[T_0,t]} \mathbf{F}(f, T_0, t)$ holds, where $\mathbf{F}(\cdot, \cdot, t)$ is defined in (2).*

Proof. The proof is a direct application of Theorem 8.8 on page 128 of Wheeden and Zygmund (1977), where $g(t-\tau) := \eta e^{-\eta(t-\tau)}$, $p := \infty$, $p' := 1$, $\frac{1}{p} + \frac{1}{p'} = 1$, and the supremum is taken over function $g(t-\tau)$, in which $\|g(t-\tau)\|_{\mathcal{L}_1} \leq 1$.

Lemma 2 (*Khargonekar, Petersen, & Zhou, 1990*)**.** *For any real matrices of appropriate dimensions M, N, constant $\varepsilon > 0$ and a time-varying matrix $\mathcal{F}(t)$ satisfying $\mathcal{F}(t)'\mathcal{F}(t) \leq I$ for any $t \geq 0$ we have $M'\mathcal{F}(t)N + N'\mathcal{F}'(t)M \preceq \varepsilon^{-1}M'M + \varepsilon N'N$.*

Definition 2 (*Permanent Abrupt Fault (Reppa et al., 2016)*)**.** Let $\theta(t)$ be the time profile, which includes the time duration and the evolution mode of occurrence or disappearance, and $\phi(t)$ be a function that represents the signature of a fault f, respectively. A permanent abrupt fault is defined as $f(t) = \theta(t)\phi(t - t_f)$, where $\phi_1 \leq |\phi| \leq \phi_2, \forall t \geq 0$, $\phi_1 \in \mathbb{R}_+$, $\phi_2 \in \mathbb{R}_+$, $\theta(t) = 0$, if $t < t_f$ or $\theta(t) = 1$ if $t \geq t_f$, where t_f is the instant of the first occurrence of the fault, formally defined as $t_f := \min\{t \in \mathbb{R}_+ : \|f(t)\| \geq \phi_1\}$.

Definition 3 (*FDI Device*)**.** An FDI device is a system composed of an observer-based residual error generator and residual-evaluation-based functions such as residual evaluation, threshold, and alarm, whose objective is to detect and isolate specific faults.

3. Problem formulation

We consider a class of continuous-time uncertain SAS subject to additive permanent abrupt sensor faults as[1]

$$\mathcal{G}_\sigma : \begin{cases} \dot{x} = (A_\sigma + \Delta A_\sigma)x + b_\sigma, \; x(0) = x_0 \\ y = C_\sigma x + F_\sigma f_s, \end{cases} \tag{3}$$

where $\sigma(\cdot) : \mathbb{R}_+ \to \mathbb{I}_\mathscr{M}$ is a piecewise constant switching signal that selects a known mode i in the set $\mathbb{I}_\mathscr{M}$, $x \in \mathbb{R}^n$ is the state, $y \in \mathbb{R}^p$ is the output, with $p < n$, $f_s \in \mathbb{R}^p$ is the sensor faults vector, corresponding to an exogenous signal that affects the output measurements, with $0 \leq \|f_s\| \leq \bar{f}_{\max}, \forall t \geq 0$, where $\bar{f}_{\max} > 0$ is a finite constant given by the designer and $f_s(0) = 0$. The matrices $A_i \in \mathbb{R}^{n\times n}$, $b_i \in^{n\times m}$, $C_i \in \mathbb{R}^{p\times n}$ and $F_i \in \mathbb{R}^{p\times p}$ represent state, input, output and fault distribution matrices, respectively and C_i is full row rank for all $i \in \mathbb{I}_\mathscr{M}$. For every $i \in \mathbb{I}_\mathscr{M}$, matrices $\Delta A_i \in \mathbb{R}^{n\times n}$ have the following form (Elias, Faria, Araujo, Magossi, & Oliveira, 2022):

$$\Delta A_i = \delta_a(t)Q_i, \;\; |\delta_a(t)| \leq \delta, \forall i \in \mathbb{I}_\mathscr{M}, \forall t \geq 0, \tag{4}$$

where $Q_i := M_iN_i$ are given for all $i \in \mathbb{I}_\mathscr{M}$, and $\delta_a : \mathbb{R} \to [-\delta, \delta]$ are unknown functions and $\delta \in [0, 1]$ is a constant to be given. The matrices $M_i \in \mathbb{R}^{n\times m_A}$, $N_i \in \mathbb{R}^{m_A\times n}$, with $m_A = \max_{i\in\mathbb{I}_\mathscr{M}}(\text{rank}(Q_i))$ are matrices that represent structured uncertainties and are obtained by using full rank factorization (Piziak & Odell, 1999).

To obtain the detection and isolation for each system sensor among a number of p sensors, the following assumptions are considered.

Assumption 1. The system in (3) is not fully available for measurements, the pairs (A_i, C_i) are observable for all $i \in \mathbb{I}_\mathscr{M}$ and each sensor fault f^ℓ for all $\ell \in \mathbb{F}$ is considered to be a permanent abrupt fault based on Definition 2, with $f = f^\ell$, $t_f = t_f^\ell$.

Assumption 2. All sensors are prone to bounded faults, all sensor faults may occur simultaneously, and for all $i \in \mathbb{I}_\mathscr{M}$, F_i are assumed to be diagonal with $\text{rank}(F_i) = p$.

Assumption 2 represents a critical condition where all sensors could be permanently damaged. Although all the sensor faults may occur simultaneously, they are independent, i.e., a fault in a sensor does not depend on the occurrence of faults in any other sensor.

Let $\mathbb{F} := \{1, \ldots, p\}$ be the set of all fault indices, and let $\mathscr{F} := \{f^\ell \in \mathbb{R} : \ell \in \mathbb{F}\}$ be the set of all sensor faults, where function $f^\ell \in \mathcal{L}_\infty, \forall \ell \in \mathbb{F}$ represents the ℓ^{th} fault function in the ℓ^{th} position of vector f_s. Since F_σ is assumed to be diagonal for any $\sigma = i, i \in \mathbb{I}_\mathscr{M}$, we split the matrices F_i in (3) into $p \times i$ different matrices $D_i^\ell \in \mathbb{R}^p$, where each D_i^ℓ matrix represents the ℓ^{th} column of F_i, such that $F_if_s = \sum_{\ell=1}^p D_i^\ell f^\ell$. Let now $d_f^\ell := \left[f^1, \ldots, f^{\ell-1}, f^{\ell+1}, \ldots f^p\right]$, $d_f^\ell \in \mathcal{L}_\infty$, $d_f^\ell \in \mathbb{R}^{p_1}$, $p_1 := p - 1$, $\ell \in \mathbb{F}$ define a vector of the remaining faults, i.e., a vector containing all faults except the ℓ^{th} fault, and let $E_i^\ell \in \mathbb{R}^{p\times p_1}$ be matrices composed by the columns of F_i except the ℓ^{th} column. The system in (3) is then rewritten as follows:

$$\mathcal{G}_\sigma^\ell : \begin{cases} \dot{x} = (A_\sigma + \Delta A_\sigma)x + b_\sigma \\ y = C_\sigma x + D_i^\ell f^\ell + E_i^\ell d_f^\ell. \end{cases} \tag{5}$$

The objective of this paper is to design a number of p FDI devices as in Definition 3, where each ℓ^{th} FDI device is designed to detect and isolate each permanent abrupt sensor fault f^ℓ even under the presence of multiple sensor faults, i.e., each fault f^ℓ must be detected. Uncertainties and remaining faults d_f^ℓ must remain undetected in the ℓ^{th} FDI device, for some uncertainty functions satisfying (4) and for any $d_f^\ell \in \mathcal{D}^\ell$, with $\mathcal{D}^\ell$ obtained as

$$\mathcal{D}^\ell = \{d_f^\ell \in \mathbb{R} : 0 \leq \|d_f^\ell\| \leq d_{\max}^\ell\}, \tag{6}$$

where $d_{\max}^\ell \leq \bar{f}_{\max}$ represents the bound of the magnitude of faults vector f_s when all sensor faults occur simultaneously, except for the ℓ^{th} fault, and constants $f_{\max}^\ell \leq \bar{f}_{\max}$ are known and represents the maximum bound of the magnitude of each sensor fault, satisfying

$$0 \leq \|f^\ell\| \leq f_{\max}^\ell. \tag{7}$$

We also propose an FDI strategy for the class of systems $\mathcal{G}_\sigma$ under a measurable switching signal σ, assuming that the solutions of the system in (3) are bounded.

3.1. Structure of the observer-based residual error generators

To obtain the bank of residual error generators in a pseudo-dedicated scheme, let $z^\ell \in \mathbb{R}^n$ and $r^\ell \in \mathbb{R}^p$ be the state estimate,

[1] For some switched power electronic systems representation, the vector b_σ in (3) can be expressed as $b_\sigma = B_\sigma u(t)$, where $u \in \mathbb{R}^m$ is an external input assumed to be constant for all $t \geq 0$ and B_σ is an input matrix. Since u is a constant vector, then b_σ is an affine term.

and a residual error signal, respectively. For each $\ell \in \mathbb{F}$, the residual error generator is designed as follows:

$$\widehat{\mathcal{G}}^{\ell}_{\sigma}: \begin{cases} \dot{z}^{\ell} = A_{\sigma} z^{\ell} + b_{\sigma} + L^{\ell}_{\sigma}(y - C_{\sigma} z^{\ell}), \\ r^{\ell} = R^{\ell}_{\sigma}(y - C_{\sigma} z^{\ell}), \end{cases} \tag{8}$$

where $L^{\ell}_i \in \mathbb{R}^{n\times p}$ are the observer gain matrices and $R^{\ell}_i \in \mathbb{R}^{p\times p}$ are gain matrices for the residual error signal, with $R^{\ell}_i \succ 0, \forall i \in \mathbb{I}_{\mathscr{M}}, \ell \in \mathbb{F}$.

Let $e^{\ell}_z = x - z^{\ell}$ denote the estimation error. Then, the dynamics of the error e^{ℓ}_z are given by

$$\begin{aligned} \dot{e}^{\ell}_z &= (A_{\sigma} - L^{\ell}_{\sigma} C_{\sigma}) e^{\ell}_z - L^{\ell}_{\sigma}\left(D^{\ell}_{\sigma} f^{\ell} + E^{\ell}_{\sigma} d^{\ell}_f\right) + \Delta A_{\sigma} x \\ r^{\ell} &= R^{\ell}_{\sigma}\left(C_{\sigma} e^{\ell}_z + D^{\ell}_{\sigma} f^{\ell} + E^{\ell}_{\sigma} d^{\ell}_f\right). \end{aligned} \tag{9}$$

Considering linear dynamics, the estimation error in (9) can be decomposed in terms of fault and remaining faults as $e^{\ell}_z := e^{\ell}_f + e^{\ell}_d$, $r^{\ell} := r^{\ell}_f + r^{\ell}_d$ and system (9) can be represented by

$$\begin{cases} \dot{e}^{\ell}_f = (A_{\sigma} - L^{\ell}_{\sigma} C_{\sigma}) e^{\ell}_f - L^{\ell}_{\sigma} D^{\ell}_{\sigma} f^{\ell} \\ r^{\ell}_f = R^{\ell}_{\sigma}\left(C_{\sigma} e^{\ell}_f + D^{\ell}_{\sigma} f^{\ell}\right), \end{cases} \tag{10}$$

$$\begin{cases} \dot{e}^{\ell}_d = (A_{\sigma} - L^{\ell}_{\sigma} C_{\sigma}) e^{\ell}_d - L^{\ell}_{\sigma} E^{\ell}_{\sigma} d^{\ell}_f + \Delta A_{\sigma} x \\ r^{\ell}_d = R^{\ell}_{\sigma}\left(C_{\sigma} e^{\ell}_d + E^{\ell}_{\sigma} d^{\ell}_f\right), \end{cases} \tag{11}$$

where pairs $(e^{\ell}_f, r^{\ell}_f), (e^{\ell}_d, r^{\ell}_d)$ represent the pairs of estimation and residual error signals regarding f^{ℓ} and d^{ℓ}_f in the presence of uncertainties, respectively, and $e^{\ell}_f(0) = 0$.

Now, define the set

$$\Omega_0 = \{x(0) \in \mathbb{R}^n : \|x(0)\|^2 \le \omega_0^2\}, \omega_0 \in [0, \infty), \tag{12}$$

with ω_0 a known constant. The initial condition of systems in (8) (9) and (11) is obtained considering $x(0) \in \Omega_0$ satisfying Assumption 3.

Assumption 3. For any initial condition $x(0) \in \Omega_0$ there exists a switching signal σ that ensures that the trajectories of system (3) are bounded.

From (12) and Assumption 3, the following set can be defined

$$\Omega_x := \{x(t) \in \mathbb{R}^n : \|x(t)\|^2 \le \overline{\omega}^2, \forall t \ge 0\}, \tag{13}$$

where $\omega_0 \le \overline{\omega}$ and $\Omega_0 \subseteq \Omega_x$, under switching signal σ. Then, the following proposition can be proved.

Proposition 1. *Consider $x(0) \in \Omega_0$ as in (12) and $\sigma(0) = \sigma_0 \in \mathbb{I}_{\mathscr{M}}$ in system (3), where σ_0 is known. By assuming that $z^{\ell}(0) := C^{\dagger}_{\sigma(0)} y(0)$, initial estimation errors $e_z(0)$ and $e_d(0)$ will also belong to Ω_0.*

Proof. Since $f_s(0)$ is assumed to be zero, an estimative for the initial condition $x(0)$ in (3), denoted by $x^*(0)$, can be found by solving the following least squares minimization problem:

$$\min_{x(0)\in\mathbb{R}^n} \|C_{\sigma(0)} x(0) - y(0)\|, \tag{14}$$

where $x^*(0) = C^{\dagger}_{\sigma(0)} y(0)$ is the optimal solution. Therefore, by making $z^{\ell}(0) := x^*(0) = C^{\dagger}_{\sigma(0)} y(0), \forall \ell \in \mathbb{F}$ we obtain:

$$\begin{aligned} \|e(0)\| := \|x(0) - z^{\ell}(0)\| &= \|x(0) - C^{\dagger}_{\sigma(0)} y(0)\| \\ &\le \|x(0)\| \le \omega_0, \end{aligned} \tag{15}$$

where inequality (15) is obtained as $z^{\ell}(0) = x^*(0) = 0$, it is the worst-case solution of the optimization problem (14). Therefore, $e_z(0) \in \Omega_0$. Moreover, from $f_s(0) = 0$, it follows that $e_f(0) = 0$, whereas $e_z(0) = e_d(0)$. Thus, we can conclude that $e_d(0) \in \Omega_0$.

The gains L^{ℓ}_i and R^{ℓ}_i of the residual error generators in (8) are designed to make the system in (10) achieves an $\mathcal{S}_-$ sensitivity performance and system (11) achieves $\mathcal{L}_\infty$ attenuation performance defined in the sequence.

Definition 4 ($\mathcal{S}_-$ *Sensitivity Performance*)**.** System in (10) has a $\mathcal{S}_-$ sensitivity performance if its trajectories are bounded and there exists a sensitivity gain $\overline{\beta} > 0$ such that $\|r^{\ell}_f\|_{\mathcal{L}_\infty} > \overline{\beta}\|f^{\ell}\|_{\mathcal{L}_\infty}, \ \forall \|f^{\ell}\|_{\mathcal{L}_\infty} \ne 0$.

Definition 5 ($\mathcal{L}_\infty$ *Performance*)**.** System in (11) has a guaranteed robust $\mathcal{L}_\infty$ attenuation performance if its trajectories are bounded and there exist positive attenuation gains $\gamma^{\ell}, \overline{\varepsilon}^{\ell}_x, \eta, \vartheta$ such that $\|r^{\ell}_d\|_{\mathcal{L}_\infty} \le \sqrt{\gamma^{\ell}\|d^{\ell}_f\|^2_{\mathcal{L}_\infty} + \overline{\varepsilon}^{\ell}_x \omega^2 + \eta\vartheta}, \forall \ell \in \mathbb{F}$, where $\omega > 0$ is a given constant satisfying

$$\Omega := \{x(t) \in \mathbb{R}^n : \max_{i\in\mathbb{I}_{\mathscr{M}}} \|N_i x(t)\|^2 \le \omega^2, \forall t \ge 0\}. \tag{16}$$

3.2. Residual-evaluation-based functions

The residual evaluation process is performed using residual evaluation functions denoted by $J^{\ell} : \mathbb{R}^p \times \mathbb{R}_+ \to \mathbb{R}_+$ which are function of each residual error signal r^{ℓ}. Threshold functions denoted by $J^{\ell}_{th} : \mathbb{R}_+ \to \mathbb{R}_+$ are designed to satisfy $J^{\ell}_{th}(t) \ge \|r^{\ell}_d(t)\|_{\mathcal{L}_\infty}, \ \forall \ell \in \mathbb{F}, \forall t \ge 0$, which means that a threshold function must be obtained so that $J^{\ell}_{th}(t)$ is greater than the maximum value of $\|r^{\ell}(t)\|$ when $\|f^{\ell}\| = 0$, $\|d^{\ell}_f\| = d^{\ell}_{\max}$ and the uncertainties are obtained for $\delta_a(t) \in [-\delta, \delta]$ that maximizes $\|N_i x(t)\|^2$, $i \in \mathbb{I}_{\mathscr{M}}$. Moreover, the output of each ℓth FDI device is a binary scalar corresponding to alarm functions as follows:

$$a^{\ell}(t) = \begin{cases} 1, & \text{if } J(r^{\ell}, t) \ge J^{\ell}_{th}(t) \\ 0, & \text{otherwise.} \end{cases} \tag{17}$$

When $a^{\ell}(t) = 1$, the fault in sensor ℓ is detected, whereas $a^{\ell}(t) = 0$, means that sensor ℓ is assumed to be fault-free. Denoting $\overline{a} \in \mathbb{R}^p$ as the output vector of the FDI device containing all alarms in each $\ell \in \mathbb{F}$ row, multiple faults are detected if $\sum_{\ell\in\mathbb{F}} a^{\ell} > 1$, and the non-zero rows of $\overline{a}$ represents a fault in the $\ell \in \mathbb{F}$th sensor. Furthermore, for a SAS under uncertainties and multiple faults, we propose a detection strategy that considers the smallest magnitude for a fault to be detected, according to the following definition, based on Reppa et al. (2017).

Definition 6. Let t^{ℓ}_f be the first time of the fault occurrence, as in Definition 2, $a^{\ell}(t) \in \{0, 1\}$ be the output of the FDI device as in (17), and $T^{\ell}_D \ge t^{\ell}_f$ be the time when the FDI device is triggered[2] by the permanent fault f^{ℓ}, satisfying

$$T^{\ell}_D := \min\{t \in [t^{\ell}_f, \infty) : a^{\ell}(t) = 1\}. \tag{18}$$

The smallest fault magnitude to be detected, of f^{ℓ}, denoted as $f^{\ell}_{\min}$ is defined as follows:

$$f^{\ell}_{\min} = \|f^{\ell}(T^{\ell}_D)\| \le f^{\ell}_{\max}. \tag{19}$$

Instead of the classical definitions as given in Blanke et al. (2016), and Reppa et al. (2018), instead of considering the detection of faults when $\|f^{\ell}\| > 0$, the strong and weak detectability definitions in this paper are obtained when $f^{\ell} \in \mathcal{F}^{\ell}_{\min}$, where $\mathcal{F}^{\ell}_{\min}$ is given by $\mathcal{F}^{\ell}_{\min} = \{f^{\ell} \in \mathbb{R} : f^{\ell}_{\min} \le \|f^{\ell}\| \le f^{\ell}_{\max}\}$, which means that the magnitude of f^{ℓ} is greater than a desired $f^{\ell}_{\min}$, with an upper bounded given by $f^{\ell}_{\max}$ whenever $f^{\ell} \in \mathcal{F}^{\ell}_{\min}$. Moreover, we consider that a small time delay in strong detection is allowed.

[2] An FDI device is triggered if its alarm function value is different from zero.

The conditions in which a fault is detected, along with the novel definitions of strong and weak detectability with respect to a given $f^\ell_{\min}$, considering alarm functions a^ℓ as in (17), t^ℓ_f, $f^\ell_{\min}$ and T^ℓ_D as in Definition 2, are given next.

Definition 7 (*Fault Detectability*). For a given $f^\ell_{\min} \in (0, f^\ell_{\max}]$, fault f^ℓ is detectable with respect to $f^\ell_{\min}$ if there exists a residual evaluation function $J(r^\ell)$, a threshold function $J^\ell_{th}(t)$ and a finite time $T^\ell_D \geq t^\ell_f$, such that $a^\ell(T^\ell_D) = 1$ when $\|f^\ell(T^\ell_D)\| = f^\ell_{\min}$.

Definition 8 (*Strong Detectability*). A fault f^ℓ is strongly detectable with respect to a given $f^\ell_{\min}$ if $f^\ell_{\min}$ is detectable, $a^\ell(t) = 1, \forall t \geq T^\ell_D$ and $f^\ell \in \mathcal{F}^\ell_{\min}, \forall t \geq T^\ell_D$.

Definition 9 (*Weak Detectability*). A fault f^ℓ is weakly detectable with respect to a given $f^\ell_{\min}$ if f^ℓ is detectable and $a^\ell(t) = 1$ only for some $t \geq T^\ell_D$ even if $f^\ell \in \mathcal{F}^\ell_{\min}$ for all $t \geq T^\ell_D$.

Complete fault isolation of f^ℓ, as defined in Blanke et al. (2016), is achieved when $a^\ell(t) = 1$ if, and only if, $\|f^\ell\| > 0$, for any $t \geq t^\ell_f$, which means that remaining faults and uncertainties must not trigger the FDI device. In this paper, we propose less restrictive conditions for fault isolation considering a given smallest fault magnitude to be detected for fault f^ℓ, as defined as follows.

Definition 10 (*Fault Isolation*). For a given $f^\ell_{\min} \in (0, f^\ell_{\max}]$, the fault isolation of a fault f^ℓ is achieved if f^ℓ is strongly detectable and $a^\ell(t) = 0, \forall t < t^\ell_f$.

When fault isolation as in Definition 10 is achieved, remaining faults and uncertainties will not trigger the FDI device, and a fault $f^\ell \in \mathcal{F}^\ell_{\min}$ is guaranteed to be detected. However, fault isolation may not be guaranteed for some range of uncertainties. In the sequence, we give the definitions of weak and strong isolation with respect to the effect of the uncertainties in the FDI devices for uncertain SAS as in (5), and uncertainties functions satisfying (4) for a $\delta \in [0, 1]$ to be found. Furthermore, in the next section, we provide the main results in the design of the FDI devices for each $f^\ell \in \mathscr{F}$.

Definition 11 (*Weak Isolation*). For a given $f^\ell_{\min}$, the weak fault isolation of a fault f^ℓ is achieved if, for any $d^\ell_f \in \mathcal{D}^\ell$, $\delta_a \in [-\delta, \delta]$, and some $\delta \in [0, 1]$ fault isolation is guaranteed.

Definition 12 (*Strong Isolation*). For a given $f^\ell_{\min}$, the strong isolation of fault f^ℓ is achieved if, for any $d^\ell_f \in \mathcal{D}^\ell$ and $\delta_a \in [-1, 1]$, fault isolation is guaranteed.

Considering the definition of $f^\ell_{\min}$, we define a novel mixed $\mathcal{S}_-/\mathcal{L}_\infty$ performance.

Definition 13 ($\mathcal{S}_-/\mathcal{L}_\infty$ *Performance*). The system in (9) has a mixed $\mathcal{S}_-/\mathcal{L}_\infty$ sensitivity/attenuation performance if its trajectories are bounded and, for a given $f^\ell_{\min} \leq f^\ell_{\max}$, there exist a positive sensitivity gain $\overline{\beta}$ and positive attenuation gains γ^ℓ, $\overline{\varepsilon}^\ell_x$, η, ϑ such that $\mathcal{S}_-$ as in Definition 4 and $\mathcal{L}_\infty$ as in Definition 5 are obtained, and weak or strong isolation are achieved.

4. Main results

The FDI strategy proposed in this work provides LMI-based conditions to achieve weak isolation of all sensors fault by first designing the residual error generators considering an optimization problem which solution gives sensitivity and attenuation guarantees and then we obtain threshold functions relying on the gains and parameters obtained as a solution of a sensitivity/attenuation optimization problem.

In Theorems 1 and 2, we provide LMI-based conditions in an optimization problem to obtain observer gains L^ℓ_i and R^ℓ_i for each sensor fault $\ell \in \mathbb{F}$ with $\mathcal{S}_-$ and $\mathcal{L}_\infty$ guarantees, respectively, whereas Theorem 3 proposes an optimization problem that satisfies the constraints in Theorem 1 and Theorem 2 simultaneously, considering uncertain functions as in (4) with $\delta = 1$. Whenever it is possible to find a feasible solution to the problem in Theorem 3, the gains and parameters obtained are used in Lemma 3 and Theorem 4 to obtain a threshold function for each $\ell \in \mathbb{F}$ to guarantee weak isolation and a mixed $\mathcal{S}_-/\mathcal{L}_\infty$ performance considering the prespecified smallest fault magnitude to be detected, denoted $f^\ell_{\min}$, and a range of uncertainties defined in (4) where $\delta \in [0, 1]$. Moreover, Corollary 1 proposes an LMI-based optimization problem to obtain the smallest fault magnitude to be detected $f^\ell_{0\min}$ such that strong isolation is guaranteed. Additionally, Theorem 5 proposes conditions to obtain piecewise constant threshold functions to relax the constraints in Theorem 4. To this end, Algorithm 1 can be applied to find the threshold functions in a structured manner. Finally, Algorithm 2 enables finding local optima observer gains and threshold functions by varying a parameter associated with the decay rate of Lyapunov-like functions.

In this section, we omit index ℓ, and the argument t in time-dependent functions when not essential to simplify the notation. However, the results obtained can be applied to all FDI devices without loss of generality.

4.1. Residual error generators design

The following theorems yield sufficient conditions in terms of LMIs to guarantee that (10) has an $\mathcal{S}_-$ performance and (11) has an $\mathcal{L}_\infty$ performance.

Theorem 1. *Consider system (10). For given positive scalar $\eta > 1$, if there exist matrices $P \in \mathbb{R}^{n\times n}$, $P \succ 0$, $H_i \in \mathbb{R}^{p\times p}$, $H_i \succeq 0$, $W_i \in \mathbb{R}^{p\times n}$ and scalars $\beta > 0$, $\eta_f > 0$ as a solution to the following optimization problem for $\sigma = i, \forall i \in \mathbb{I}_{\mathscr{M}}$ a*

$$\max_{P,W_i,H_i,\beta,\eta_f} \beta, \text{ s.t.} \tag{20}$$

$$\Lambda_i \prec 0 \tag{21}$$

$$\Psi_i \prec 0, \tag{22}$$

where $\psi^i_{11} = He(A_iP + C_i'W_i) + \eta P - C_i'H_iC_i$ and

$$\Lambda_i = \begin{bmatrix} (-\eta+1)P + C_i'H_iC_i & C_i'H_iD_i \\ \star & D_i'H_iD_i - \beta I - \eta_f f^{-2}_{\max} I \end{bmatrix} \tag{23}$$

$$\Psi_i = \begin{bmatrix} \psi^i_{11} & \star \\ D_i'W_i - D_i'H_iC_i & \beta I - D_i'H_iD_i \end{bmatrix}, \tag{24}$$

then under $e_f(0) = 0$, the trajectories of (10) are bounded with respect to

$$\Omega_f = \left\{ e_f \in \mathbb{R}^n : \|e_f\|_{\mathcal{L}_\infty} < \sqrt{\eta_f(\lambda_{\min}(P))^{-1}} \right\},$$

and (10) has a guaranteed $\mathcal{S}_-$ performance with a maximum sensitivity gain. In addition, the observer gain matrices L_i, R_i for each $i \in \mathbb{I}_{\mathscr{M}}$ are obtained by $L_i = -(W_iP^{-1})'$ and $R_i = H_i^{1/2}$.

Proof. Let a $\mathcal{C}^1$ function be $V := e_f'Pe_f$, an augmented vector be $\chi := \left[e_f', f'\right]'$ and define $W_i := -L_i'P$, $H_i := R_i'R_i$. The time derivative of V is given by $\dot{V} = \chi'\Psi_\sigma\chi - \eta V + \|r_f\|^2 - \beta\|f\|^2$, where $\|r_f\|^2 = e_f'C_\sigma'H_\sigma C_\sigma e_f + 2f'(D_\sigma'H_\sigma C_\sigma)e_f + f'(D_\sigma'H_\sigma D_\sigma)f$, and Ψ_σ is given in (22) for all $\sigma = i, i \in \mathbb{I}_{\mathscr{M}}$. When (22) holds, the following inequality is satisfied:

$$\dot{V} < -\eta V + \|r_f\|^2 - \beta\|f\|^2. \tag{25}$$

From (25), is not yet possible to guarantee the stability of (10), since $\|r_f\|^2 \geq 0$ and the negativity of $\dot{V}$ is not ensured. Thus, to guarantee that the trajectories of e_f are attracted to Ω_f, it is added in inequality (25) the null term $-V+V-\eta_f f_{\max}^{-2}\|f\|^2+\eta_f f_{\max}^{-2}\|f\|^2$, yielding:

$$\dot{V} < -\eta V + \|r_f\|^2 - \beta\|f\|^2 = \chi'\Lambda_i\chi - V + \frac{\eta_f}{f_{\max}^2}\|f\|^2,$$

where Λ_i is defined in (23). By satisfying (21), it follows that

$$\begin{aligned}\dot{V} &< -\eta V + \|r_f\|^2 - \beta\|f\|^2 < -V + \eta_f f_{\max}^{-2}\|f\|^2 \\ &< -V + \eta_f.\end{aligned} \tag{26}$$

Therefore, from (26), $\dot{V} < 0$ whenever $e_f \notin \Omega_f$. Also, by integrating (26) from 0 to t, we obtain

$$V(t) < e^{-t}V(0) + \eta_f\int_0^t e^{-(t-\tau)}d\tau. \tag{27}$$

Hence, under null initial conditions, the trajectories of (10) are bounded with respect to Ω_f. Moreover, by integrating (25) from 0 to t, we obtain:

$$V(t) < e^{-\eta t}V(0) + \mathbf{G}(\|r_f\|^2, t) - \beta\mathbf{G}(\|f\|^2, t), \tag{28}$$

with $\mathbf{G}(\cdot, t)$ as in Definition 1. Since $V \geq 0, \forall t \geq 0$, inequality (28) is satisfied whenever

$$\beta\mathbf{G}(\|f\|^2, t) < \mathbf{G}(\|r_f\|^2, t). \tag{29}$$

Multiplying both sides of (29) to η and applying the supremum on both sides of (29) yields:

$$\beta\eta \sup_{[0,t]}\mathbf{G}(\|f\|^2, t) < \eta \sup_{[0,t]}\mathbf{G}(\|r_f\|^2, t). \tag{30}$$

Applying Lemma 1 in (30), we guarantee that the residual signal r_f in (10) has an $\mathcal{S}_-$ sensitivity performance as in Definition 4 with $\overline{\beta} = \sqrt{\beta}$, where $\overline{\beta}$ is the maximum sensitivity gain obtained by the maximization of β.

Theorem 2. *Consider the system in (11) and Assumption 3. For given positive scalars η, ω satisfying (16), and $e_d(0) \in \Omega_0$, if there exist matrices $P \in \mathbb{R}^{n\times n}, P \succ 0$, $H_i \in \mathbb{R}^{p\times p}, H_i \succeq 0$, $W_i \in \mathbb{R}^{p\times n}$, and positive scalars ε_{xi}, γ as solution to the following convex optimization problem for all $\sigma = i, i \in \mathbb{I}_{\mathscr{M}}$:*

$$\min_{P,W_i,H_i,\varepsilon_{xi},\varepsilon_{xi}} \gamma \tag{31}$$

$$\text{s.t. } \eta - \gamma d_{\max}^2 - \varepsilon_{xi}\omega^2 \geq 0, \text{ and} \tag{32}$$

$$\begin{bmatrix} \Theta_{11}^i & W_i'E_i & PM_i \\ \star & -\gamma I + E_i'H_iE_i & 0 \\ \star & \star & -\varepsilon_{xi}I \end{bmatrix} \prec 0, \tag{33}$$

where $\Theta_{11}^i = He(A_i'P + C_i'W_i) + \eta P + C_i'H_i'C_i$, then, the trajectories of (11) are bounded with respect to

$$\Omega_d = \left\{e_d \in \mathbb{R}^n : \|e_d\|_{\mathcal{L}_\infty} < ((\vartheta+1)/\lambda_{\min}(P))^{1/2}\right\}$$

where $\vartheta := \lambda_{\max}(P)\omega_0^2$, with ω_0 obtained considering Proposition 1. Furthermore, the $\mathcal{L}_\infty$ performance of (11) is guaranteed. In addition, the observer gain matrices L_i, R_i for each $i \in \mathbb{I}_{\mathscr{M}}$ are obtained by $L_i = -(W_iP^{-1})'$ and $R_i = H_i^{1/2}$.

Proof. Let a $\mathcal{C}^1$ function be defined as $V = e_d'Pe_d$, an augmented vector be $\chi := \left[e_d', d_f'\right]'$ and define $W_i := -L_i'P$, $H_i := R_i'R_i$. The time derivative of V satisfies

$$\begin{aligned}\dot{V} &= e_d'(\text{He}(A_\sigma'P + C_\sigma'W_\sigma))e_d + 2e_d'W_\sigma'E_\sigma d_f \\ &\quad + 2e_d'P\Delta A_\sigma x \\ &\leq \chi'\Phi_\sigma\chi - \eta V - \|r_d\|^2 + \varepsilon_{x\sigma}\|N_\sigma x\|^2 + \gamma\|d_f\|^2,\end{aligned} \tag{34}$$

where the inequality in (34) is obtained by applying Lemma 2 in $2e_d'(P\Delta A_\sigma)x$, $\|r_d\|^2 = e_d'C_\sigma'H_\sigma'C_\sigma e_d + 2e_d'(C_\sigma'H_\sigma E_\sigma)d_f + d_f{}'E_\sigma'H_\sigma E_\sigma d_f$ and Φ_σ is defined as

$$\Phi_\sigma = \begin{bmatrix} \Phi_{11}^\sigma & W_\sigma'E_\sigma + E_\sigma'H_\sigma E_\sigma \\ \star & -\gamma I + E_\sigma'H_\sigma E_\sigma \end{bmatrix}, \tag{35}$$

with $\Phi_{11}^\sigma := \text{He}(A_\sigma'P + C_\sigma'W_\sigma) + \varepsilon_{x\sigma}^{-1}PM_\sigma M_\sigma'P + \eta V + C_\sigma'H_\sigma C_\sigma$. By applying Schur's complement in (35), we obtain (33), and by solving (31)–(33) the derivative V in (34), satisfies

$$\dot{V} < -\eta V - \|r_d\|^2 + \gamma\|d_f\|^2 + \varepsilon_{x\sigma}\|N_\sigma x\|^2 \tag{36}$$

$$\dot{V} < -\eta V - \|r_d\|^2 + \gamma\|d_f\|^2 + \overline{\varepsilon}_x\omega^2 \tag{37}$$

$$\leq -\eta V - \|r_d\|^2 + \gamma d_{\max}^2 + \overline{\varepsilon}_x\omega^2, \tag{38}$$

where $\overline{\varepsilon}_x := (\max_{i\in\mathbb{I}_{\mathscr{M}}}(\varepsilon_{xi}))$. Inequality (36) is obtained when LMI (33) is solved, whereas inequality (37) is obtained considering (16). Moreover, (38) is obtained from (6), where $\|d_f\|^2 \leq d_{\max}^2$. Furthermore, applying the solution of (32) in (38), we obtain:

$$\dot{V} < -\eta V - \|r_d\|^2 + \eta < -\eta V + \eta. \tag{39}$$

By (39), we ensure that $\dot{V} < 0$ whenever $\|e_d\| \geq \lambda_{\min}(P)^{-1/2}$. Moreover, by integrating (39) from 0 to t, the following inequalities are satisfied:

$$\begin{aligned}V(t) &< e^{-\eta t}(V(0) - 1) + 1 < e^{-\eta t}V(0) + 1 \\ &\leq e^{-\eta t}\vartheta + 1,\end{aligned}$$

considering $\vartheta = \lambda_{\max}(P)\omega_0^2$. Hence, for any $d_f \in \mathcal{D}_f$, $\delta_a \in [-1, 1]$ and $e_d(0) \in \Omega_0$, the trajectories of (11) are bounded with respect to Ω_d. Moreover, by integrating (37), we have:

$$\begin{aligned}V(t) &< e^{-\eta t}V(0) - \mathbf{G}(\|r_d\|^2, t) \\ &\quad + \mathbf{G}(\gamma\|d_f\|^2 + \overline{\varepsilon}_x\omega^2, t).\end{aligned} \tag{40}$$

In addition, $V \geq 0, \forall t \geq 0$. Therefore, from inequality (40) the following inequality is obtained

$$\mathbf{G}(\|r_d\|^2, t) < \mathbf{G}\big(\gamma\|d_f\|^2 + \overline{\varepsilon}_x\omega^2, t\big) + e^{-\eta t}\vartheta. \tag{41}$$

Applying the supremum and multiplying by η both sides of (41), yields:

$$\begin{aligned}&\eta\sup_{[0,t]}\mathbf{G}(\|r_d\|^2, t) < \\ &\eta\sup_{[0,t]}(\mathbf{G}\big(\gamma\|d_f\|^2 + \overline{\varepsilon}_x\omega^2, t\big) + e^{-\eta t}\vartheta) \\ &\leq \gamma\|d_f\|_{\mathcal{L}_\infty}^2 + \overline{\varepsilon}_x\omega^2 + \eta\vartheta.\end{aligned} \tag{42}$$

Finally, applying Lemma 1 in (42), the $\mathcal{L}_\infty$ in Definition 5 is obtained.

When the $\mathcal{L}_\infty$ performance is guaranteed, the effect of the remaining faults in the residual error signal is attenuated. However, the sensitivity to a certain fault must be guaranteed. In the following theorem, we propose a combined solution of $\mathcal{S}_-$ and $\mathcal{L}_\infty$ performances to enhance the detection capabilities of the residual error generator in the presence of a single sensor fault, whereas the effect of the remaining faults and uncertainties is attenuated.

Theorem 3. *Consider systems (9), (10) and (11) and Assumption 3. For given positive scalar $\eta > 1$, ω satisfying (16), and $e_d(0) \in \Omega_0$, if there exist matrices $P \in \mathbb{R}^{n\times n}, P \succ 0$, $H_i \in \mathbb{R}^{p\times p}, H_i \succ 0$, $W_i \in \mathbb{R}^{p\times n}$ and positive scalars $\beta, \eta_f, \varepsilon_{xi}, \gamma$ as a solution to the following optimization problem for all $\sigma = i, i \in \mathbb{I}_{\mathscr{M}}$:*

$$\min_{P,W_i,H_i,\beta,\eta_f,\gamma,\varepsilon_{xi}} \gamma - \beta, \tag{43}$$

$$\text{s.t. (21), (22), (32), and (33)} \tag{44}$$

then under $e_f(0) = 0$ and $e_z(0) = e_d(0)$, the trajectories of system (9) are bounded with respect to

$$\Omega_{fd} := \left\{ e_z \in \mathbb{R}^n : \|e_z\|_{\mathcal{L}_\infty} < \frac{(\sqrt{\eta_f} + \sqrt{(\vartheta+1)})}{\sqrt{\lambda_{\min}(P)}} \right\}.$$

where $\vartheta := \lambda_{\max}(P)\omega_0^2$, with ω_0 obtained considering Proposition 1. Furthermore, the system in (10) has a guaranteed $\mathcal{S}_-$ performance according to Definition 4, whereas (11) has a guaranteed $\mathcal{L}_\infty$ performance, according to Definition 5. In addition, the observer gain matrices L_i, R_i for each $i \in \mathbb{I}_{\mathscr{M}}$ are obtained by $L_i = -(W_iP^{-1})'$ and $R_i = H_i^{1/2}$.

Proof. The proof is straightforward using the same steps as in Theorems 1 and 2, considering a $\mathcal{C}^1$ function $V(e_z) = V(e_f)+V(e_d)$.

Remark 1. The value of ω satisfying (16) corresponds to the application of a switching signal σ in (3) with an initial condition $x(0)$ in the set Ω_0 and satisfying Assumption 3. If any other σ is considered, the results obtained in Theorems 2 and 3 are still valid whenever inequalities (12) and (16) hold. Nonetheless, if another ω or ω_0 are considered, the solutions of the optimization problem in Theorems 2 and 3 are valid if the new values of ω or ω_0 are less or equal to the ω or ω_0 considered previously, respectively. If the new values of ω or ω_0 are greater than the ones considered before, then the optimization problem in Theorem 2 must be solved again, and a new solution is not always guaranteed.

Remark 2. Although the choice of greater values of ω and ω_0 implies in more relaxed conditions to obtain σ that satisfies Assumption 3, the $\mathcal{L}_\infty$ attenuation performance as in Definition 5 is reduced as ω or ω_0 increases, since the upper bound of ω is increased when ω is chosen to satisfy $\omega^2 = \bar{\lambda}_{\max}(N_i'N_i)\overline{\omega}^2$ in (16)[3] and $\vartheta = \lambda_{\max}(P)\omega_0^2$ as defined in Theorem 2. Therefore, if the solutions to the optimization problem in Theorems 2 and 3 remain valid for sufficiently large values of ω and ω_0, then the influence of residual faults and uncertainties in the error signal will be amplified, making fault isolation increasingly difficult to achieve, as the threshold functions are designed to satisfy $J_{th}^{\ell}(t) \geq \|r_d^{\ell}(t)\|_{\mathcal{L}_\infty}$, and the magnitude of $\|r_d^{\ell}(t)\|_{\mathcal{L}_\infty}$ grows when a wider range of uncertainties and initial conditions is taken into account.

Although the $\mathcal{S}_-$ and $\mathcal{L}_\infty$ performances individually are appropriate to obtain the observer gains L_i and R_i, a mixed $\mathcal{S}_-/\mathcal{L}_\infty$ performance as in Definition 13 is achieved only by proper choice of the residual evaluation function $J(\cdot)$ and threshold function $J_{th}(\cdot)$ for a given $f_{\min}$, especially under simultaneous faults.

In the next section, we propose a method to obtain $J_{th}(\cdot)$ such that weak isolation is guaranteed for a range of uncertainties satisfying $\delta_a \in [-\delta, \delta]$ and for all $d_f \in \mathcal{D}_f$ and a mixed $\mathcal{S}_-/\mathcal{L}_\infty$ performance as in Definition 13 is guaranteed.

4.2. Residual-evaluation-based functions design

Let a residual evaluation function be defined as

$$J(r,t) = \begin{cases} \sup\limits_{[t-T,t]} \|r\|, & \forall t \geq T, \\ \|r\|, & \forall t < T \end{cases} \tag{45}$$

where $T > 0$ is a finite time and (45) represents a residual evaluation function obtained as the maximum value of a residual error signal $\|r\|$ during each time interval $[t-T, t]$.

[3] Using the Rayleigh–Ritz property, $\max\limits_{i\in\mathbb{I}_{\mathscr{M}}} \|N_ix\|^2 = \max\limits_{i\in\mathbb{I}_{\mathscr{M}}}(x'(N_i'N_i)x) \leq \max\limits_{i\in\mathbb{I}_{\mathscr{M}}}(\lambda_{\max}(N_i'N_i))\|x\|^2 \leq \bar{\lambda}_{\max}(N_i'N_i)\overline{\omega}^2$, where the last inequality is obtained considering (13).

The next lemma provides sufficient conditions for a fault f to be detected using a constant threshold function $J_{th}(t)$, denoted $\bar{J}_{th}$, such that $J_{th}(t) = \bar{J}_{th}$, $\forall t \geq 0$ and a residual evaluation function satisfying (45).

Lemma 3. *Consider systems (9), (10), and (11), functional $\mathbf{F}(\cdot,\cdot,\cdot)$ defined in (2), $e_d(0) \in \Omega_0$ and consider positive constants $d_{\max}$ and $f_{\max}$ satisfying (6) and (7), respectively. For an interval $t \in [T_0, T_1)$, if there exists positive constants $\beta, \gamma, \bar{\varepsilon}_x, \eta, \omega, \vartheta, f_{\min}, \alpha \in [0, 1]$, and a fault f such that the following inequalities are satisfied*

$$\mathbf{F}(\|r_f\|^2, T_0, t) \geq \beta\mathbf{F}(\|f\|^2, T_0, t) \tag{46}$$

$$\mathbf{F}(\|r_d\|^2, T_0, t) \leq \gamma\mathbf{F}(\|d_f\|^2, T_0, t) + \alpha\mathbf{F}(\bar{\varepsilon}_x\omega^2, T_0, t) + e^{-\eta T_0}\vartheta \tag{47}$$

$$f_{\min} \leq f_{\max} \tag{48}$$

$$\inf_{[T_D,t]} \|f\|^2 = f_{\min}^2 \tag{49}$$

$$\alpha \leq \frac{\beta f_{\min}^2 - (1+\sqrt{2})^2\left(\gamma d_{\max}^2 + \eta e^{-\eta T_0}\vartheta\right)}{(1+\sqrt{2})^2\bar{\varepsilon}_x\omega^2}, \tag{50}$$

then by considering the threshold

$$\bar{J}_{th} = \sqrt{\gamma d_{\max}^2 + \alpha\bar{\varepsilon}_x\omega^2 + \eta e^{-T_0}\vartheta}, \tag{51}$$

and residual evaluation function (45), fault f is detected during the interval $t \in [T_0, T_1)$ where, $T_0 \leq T_D < T_1$ and T_D is the first time in which $\|f\| \geq f_{\min}$.

Proof. For the time interval $T_0 \leq T_D < t < T_1$, considering (46) and (49) we obtain

$$\begin{aligned} \mathbf{F}(\|r_f\|^2, T_0, t) &> \beta \inf_{[T_D,t]} \|f\|^2 \int_{T_0}^{t} e^{\eta(t-\tau)}d\tau \\ &\geq \beta f_{\min}^2\mathbf{F}(1, T_0, t), \end{aligned} \tag{52}$$

then the following inequality is satisfied

$$\sup_{[T_0,t]} \|r_f\|^2 > \beta f_{\min}^2, \forall t \in [T_0, T_1), \tag{53}$$

whenever $f \in \mathscr{F}_{\min}$. Also, by applying the supremum in both sides of (47) we have

$$\sup_{[T_0,t]} \|r_d\|^2 \leq \bar{J}_{th}^2, \forall t \in [T_0, T_1). \tag{54}$$

Since $r = r_f + r_d$, under no remaining faults and uncertainties during a time interval $t \in [T_0, T_1)$, we have $\|r\| = \|r_f\|$ in (53), and a fault is detected for any $f_{\min}$ that satisfies $\beta f_{\min}^2 \geq \bar{J}_{th}^2$. Also, if for the time interval $t \in [T_0, T_1)$ only remaining faults and uncertainties are present, then $\|r\| = \|r_d\|$ in (54), and no fault will be detected for any α in threshold (51) that satisfies (47). However, under uncertainties and multiple faults, strong or weak detectability and isolation of fault f are guaranteed only if $J(r,t) = \sup\limits_{[t-T,t]} \|r\| \geq \bar{J}_{th}$ holds whenever $f \in \mathscr{F}_{\min}$, where $\|r_f\| \neq 0$ and $\|r_d\| \neq 0$. From norm properties the equality $\|r\|^2 = \|r_f\|^2 + 2r_f{}'r_d + \|r_d\|^2$ holds. Therefore, a fault is detected when

$$\bar{J}_{th}^2 \leq \|r_f\|^2 + 2r_f{}'r_d + \|r_d\|^2 \leq \sup_{[T_0,t]} \|r\|^2, \tag{55}$$

implying that the following inequality must hold:

$$\|r_f\|^2 \geq \bar{J}_{th}^2 - 2r_f{}'r_d - \|r_d\|^2, \forall t \in [T_0, T], \tag{56}$$

which is satisfied whenever $\|r_f\|^2 \geq \bar{J}_{th}^2 + 2|r_f{}'r_d|$. Also, $2|r_f{}'r_d| \leq 2\|r_f\|\|r_d\|$ from the Cauchy-Schwartz inequality, and $2\|r_f\|\|r_d\| \leq$

$2\|r_f\|\bar{J}_{th}$ from (54). Hence (56) holds for any r_f, r_d and $\bar{J}_{th}$ satisfying

$$\|r_f\|^2 - \bar{J}_{th}^2 - 2\|r_f\|\bar{J}_{th} \geq 0. \tag{57}$$

The equality in (57) is obtained as $\|r_f\| = (1 \pm \sqrt{2})\bar{J}_{th}$. Since $\|r_f\|$ is always positive, then (57) holds whenever

$$\|r_f\|^2 \geq (1+\sqrt{2})^2 \bar{J}_{th}^2. \tag{58}$$

Multiplying both sides of (55) and (58) by $e^{-\eta(t-\tau)}$ and integrating with respect to τ from T_0 to t we obtain

$$\mathbf{F}\left(\bar{J}_{th}^2, T_0, t\right) \leq \mathbf{F}\left(\sup_{[T_0,t]}\|r\|^2, T_0, t\right) \tag{59}$$

$$\mathbf{F}\left(\|r_f\|^2, T_0, t\right) \geq \mathbf{F}\left(((1+\sqrt{2})\bar{J}_{th})^2, T_0, t\right). \tag{60}$$

From (46) and (49), inequality (60) holds whenever $\beta f_{\min}^2 \mathbf{F}(1, T_0, t) \geq \mathbf{F}(((1+\sqrt{2})\bar{J}_{th})^2, T_0, t)$ is satisfied for any time $t \in [T_0, T_1)$ and $\beta f_{\min}^2 \geq \left((1+\sqrt{2})^2(\gamma d_{\max}^2 + \alpha\bar{\varepsilon}_x\omega^2 + \eta e^{-\eta t}\vartheta)\right)$, which is obtained whenever (50) holds, since $\eta e^{-\eta T_0}\vartheta \geq \eta e^{-\eta t}\vartheta$, $\forall t \geq T_0$. Moreover when (50) is satisfied, (55) and consequently (59) holds. Finally, under any $T_0 = t - T$ for every $t \in [T_0, T_1)$, with $T_1 \geq t + T$, $T_0 \geq t_f + T$ and $0 \leq T < \infty$ the inequality $J(r,t) = \sup_{[t-T,t]}\|r\| = \sup_{[T_0,t]}\|r\| \geq \bar{J}_{th}$ is obtained, which means that the fault will be detected in a finite time.

As the faults are considered to be abrupt and permanent, $J(r,t)$ will be permanently affected and $\|f(t)\| \geq f_{\min}$ almost instantaneously, which means that $J(r,t) \geq \bar{J}_{th}$ in a short time if $\bar{J}_{th}$ satisfying $J_{th}(t) = \bar{J}_{th}, \forall t \geq 0$ is obtained guaranteeing the conditions for Lemma 3, and the fault will be detected.

In what follows, we assume that Theorem 3 was solved and matrices P, H_i, W_i and positive scalars $\beta, \eta_f, \bar{\varepsilon}_x, \gamma, \vartheta$ are known. The next theorem provides the necessary conditions to achieve strong and weak detectability and isolation of a fault f with respect to a given $f_{\min}$ for a range of uncertainties as in (4), by considering the sensitivity and attenuation gains obtained in Theorem 3.

Theorem 4 (*Weak isolation*). *For a given $f_{\min}$ satisfying (48), if there exists scalars $\alpha \in [0,1]$, $\delta \in [0,1]$ as a solution to the following optimization problem for all $t \geq 0$*

$$\max_{\alpha,\delta} \delta \tag{61}$$

subject to (50) and (62)

$$\begin{bmatrix} -\alpha\varepsilon_{xi}^{-1}PM_iM_i'P & \delta PQ_i \\ \star & -\alpha\varepsilon_{xi}N_i'N_i \end{bmatrix} \preceq 0, \tag{63}$$

then, for any fault satisfying $f \in \mathscr{F}_{\min}, \forall t \geq t_f$, by considering the residual evaluation function (45), the threshold function (51) guarantees the weak isolation of fault f if $-\delta \leq \delta_a \leq \delta, \forall t \geq 0$, where δ represents the maximum range of δ_a. Moreover, if the solution of the optimization problem results in $\delta = 1$, then strong isolation of fault f is guaranteed. Furthermore, a mixed $\mathcal{S}_-/\mathcal{L}_\infty$ performance as in Definition 13 is achieved.

Proof. Let $V(e_z)$ be the $\mathcal{C}^1$ function considered in Theorem 3. Thus, the derivatives of $V(e_z)$ satisfy:

$$\begin{aligned}\dot{V}(e_z) = \chi\Psi_\sigma\chi - \eta V + \|r_f\|^2 - \beta\|f\|^2 + 2e_d'(P\Delta A_\sigma)x \\ + e_d'(\mathrm{He}(A_\sigma'P + C_\sigma'W_\sigma))e_d + 2e_d'(W_\sigma'E_\sigma)d_f,\end{aligned} \tag{64}$$

for all $t \geq 0$. Now, suppose that at some time interval $T_0 \leq t < T_1$, the following inequality holds:

$$\begin{aligned}2e_d(t)'(P\Delta A_\sigma)x(t) \leq \alpha(\varepsilon_{x\sigma}x(t)'N_\sigma'N_\sigma x(t) \\ + \varepsilon_{xi}^{-1}e_d(t)'PM_\sigma'M_\sigma Pe_d(t)),\end{aligned} \tag{65}$$

where $\alpha \in [0,1]$. Considering the uncertain function as in (4), let (65) be rewritten as

$$\zeta'\begin{bmatrix} -\alpha\varepsilon_{x\sigma}^{-1}PM_\sigma M_\sigma'P & \delta_a PQ_\sigma \\ \star & -\alpha\varepsilon_{x\sigma}N_\sigma'N_\sigma \end{bmatrix}\zeta \preceq 0, \tag{66}$$

where $\zeta := [e_d, x]'$. By denoting $\delta = \min_{i\in\mathbb{I}_\mathscr{M}}|\delta_a|$, inequality (66) is satisfied whenever (63) holds since the eigenvalues that satisfy (63) does not change if δ_a is positive or negative for any $\sigma = i, \forall i \in \mathbb{I}_\mathscr{M}$, which means that (65) is satisfied for any time interval in which $\delta_a(t) \in [-\delta, \delta]$, $\forall i \in \mathbb{I}_\mathscr{M}$. Moreover, the derivatives of $V(e_z)$ for any $t \in [T_0, T_1)$ satisfies:

$$\begin{aligned}\dot{V}(e_z) \leq \chi'\Psi_\sigma\chi - \eta V(e_z) + \|r_f\|^2 - \beta\|f\|^2 + \\ + \chi'\tilde{\Phi}_\sigma\chi - \|r_d\|^2 + \alpha\varepsilon_{x\sigma}\|N_\sigma x\|^2 + \gamma\|d_f\|^2,\end{aligned}$$

where $\tilde{\Phi}_\sigma$ is similar to Φ_σ defined in (35), but with $\Phi_{11}^\sigma := \mathrm{He}(A_\sigma'P + C_\sigma'W_\sigma) + \alpha(\varepsilon_{x\sigma}^{-1}PM_\sigma M_\sigma'P) + \eta V + C_\sigma'H_\sigma C_\sigma$. Since (33) in Theorem 2 is satisfied, then $\Phi_i \prec 0$ for any $\alpha \in [0,1]$ and $i \in \mathbb{I}_\mathscr{M}$. Hence, by considering the solution of the optimization problem (43)–(44) in Theorem 3, the following inequalities hold:

$$\begin{aligned}\dot{V}(e_z) \leq &-\eta V(e_z) + \|r_f\|^2 - \beta\|f\|^2 - \|r_d\|^2 \\ &+ \gamma\|d_f\|^2 + \alpha\varepsilon_{x\sigma}\omega^2, \forall t \in [T_0, T_1).\end{aligned} \tag{67}$$

By integrating (67) from T_0 to t with $t \in [T_0, T_1)$ we obtain:

$$\begin{aligned}V(e_z(t)) \leq\ & e^{-\eta(t-T_0)}V(e_z(T_0)) + \mathbf{F}(\|r_f\|^2, T_0, t) \\ &- \beta\mathbf{F}(\|f\|^2, T_0, t) - \mathbf{F}(\|r_d\|^2, T_0, t) \\ &+ \gamma\mathbf{F}(\|d_f\|^2, T_0, t) + \alpha\varepsilon_{x\sigma}\omega^2\mathbf{F}(1, T_0, t).\end{aligned}$$

Under $e_z(T_0 = 0) = e_d(0)$, inequalities (46) and (47) in Lemma 3 hold. Also, by Lemma, 3 when (50) is satisfied, then the fault f is detected. Since α is obtained to satisfy (50) and (63), then for all $d_f \in \mathcal{D}_f$, if $\delta_a \in [-\delta, \delta]$ then (65) holds for all $t \geq 0$, and weak isolation of fault f with respect to $f_{\min}$ as in Definition 11 is achieved considering residual evaluation and threshold functions (45) and (51), respectively. Moreover, by (61), we obtain the maximum range $\delta_{ai} \in [-\delta, \delta]$. Furthermore, if $\delta = \alpha = 1$ is a solution of (61)–(63), then by Lemma 2, inequality (65) holds for all $\delta_{ai} \in [-1, 1]$, $i \in \mathbb{I}_\mathscr{M}$, $\forall t \geq 0$. Therefore, strong isolation of f as in Definition 12 is guaranteed. Additionally, the parameters $\beta, \gamma, \bar{\varepsilon}_x, \omega, \eta$ and ϑ guarantee $\mathcal{S}_-$, $\mathcal{L}_\infty$ performances and weak or strong isolation, thus a mixed $\mathcal{S}_-/\mathcal{L}_\infty$ is obtained.

Remark 3. Based on the results obtained in Theorem 4, for $\delta < 1$, and for all $d_f \in \mathcal{D}_f$, if $-\delta \leq \delta_a \leq \delta$ holds for all $t \in [t_f, T_D]$, but $\delta_a \notin [-\delta, \delta]$ for some $t < t_f$, weak or strong isolation is not achieved. Moreover, if the optimization problem in Theorem 4 is not feasible, then there is no guarantee that a fault will be detected. However, fault f is guaranteed to be detected if $\|f(T_D)\| = f_{\min}$, whereas weak detectability is achieved if $\|f(t)\| \geq f_{\min}$, and $-\delta < \delta_a < \delta$ for all $t \in [t_f, T_D]$ and for some $t > T_D$. On the other hand, if $-\delta \leq \delta_a \leq \delta$ holds for all $t \geq t_f$, then (65) holds for all $t \geq T_D \geq t_f$ which is sufficient to guarantee strong detectability for any sensor fault satisfying the inequality $\|f(t)\| \geq f_{\min}, \forall t \geq T_D$.

The optimization proposed in Theorem 4 aims to find the maximum range of δ_a for a given $f_{\min}$ such that weak or strong isolation is guaranteed for any $\sigma = i, \forall i \in \mathbb{I}_\mathscr{M}$. However, it is challenging to guarantee strong isolation of faults with small magnitude, since the right-hand side of constraint (50) decreases as $f_{\min}$ also decreases. On the other hand, if the designer aims to guarantee strong isolation without specifying $f_{\min}$, the smaller fault magnitude to be detected can be obtained by considering $\delta = 1$ and $f_{\min}{}^2 \leq f_{\max}^2$ in Theorem 4, as presented in the following corollary.

Corollary 1 (*Strong Isolation*). *Considering $\delta = 1$ in (4), and $\bar{f}_{\min} := f_{0\min}^2$, where $f_{0\min}$ is the smallest fault magnitude to be detected, if there exists $\alpha \in [0, 1], \bar{f}_{\min}$ as a solution of the following optimization problem*

$$\min_{\alpha, \bar{f}_{\min}} \bar{f}_{\min} \tag{68}$$

subject to (50), (63) and (69)

$$\bar{f}_{\min} \leq f_{\max}^2, \tag{70}$$

then, by considering the residual evaluation function (45), the threshold (51) guarantees the strong isolation of fault f for any fault satisfying $f \in \mathscr{F}_{\min}, \forall t \geq t_f$, with $f_{0\min} = \sqrt{\bar{f}_{\min}}$.

Proof. The proof is directly obtained by the proof of Theorem 4, considering $\delta = 1$. Inequality (70) is necessary to guarantee that $f_{0\min} \in \mathscr{F}_{\min}$.

Theorem 4 provides weak or strong isolation guarantees for all $t \geq 0$, whereas Corollary 1 provides strong isolation guarantees at the cost of increasing the value of $f_{\min}$ to the value $f_{0\min}$. However, the threshold in (51) can be conservative, since it is obtained considering the influence of the initial estimation error in the residual evaluation function, which can reduce the $\mathcal{L}_\infty$ performance as stated in Remark 2 and also results in low values of δ or high values of $f_{\min}$ when applying Theorem 4 and Corollary 1 respectively. Thus, to reduce the conservativeness of J_{th} and enhance FDI, we can consider a piecewise constant threshold, such that

$$J_{th}(t) = \begin{cases} \sqrt{\gamma d_{\max}^2 + \alpha_0 \bar{\varepsilon}_x \omega^2 + \eta \vartheta}, \forall t \in [0, T_s), \\ \sqrt{\gamma d_{\max}^2 + \alpha_1 \bar{\varepsilon}_x \omega^2 + \eta e^{-\eta T_s} \vartheta}, \forall t \geq T_s, \end{cases} \tag{71}$$

where parameters $\alpha_0 \in [0, 1]$, $\alpha_1 \in [0, 1]$ and T_s are to be designed. The following theorem provides the parameter α_1 and instant T_s that guarantees weak isolation for a given $f_{\min}$ and α_0.

Theorem 5. *For given $\mu \in (0, 1]$, and $\alpha_0 \in [0, 1]$, such that*

$$J(r, t) < \sqrt{\gamma d_{\max}^2 + \alpha_0 \bar{\varepsilon}_x \omega^2 + \eta e^{-\eta T_0} \vartheta}, \forall t < T_s, \tag{72}$$

if there exists scalars $\alpha_1 \in [0, 1]$, $\delta \in [0, 1]$ as a solution to the following optimization problem

$$\max_{\alpha_1, \delta} \delta \tag{73}$$

subject to LMI (63) with $\alpha = \alpha_1$ and (74)

$$\alpha_1 \leq \frac{\beta f_{\min}^2 - (1+\sqrt{2})^2 (1+\mu)^2 \gamma d_{\max}^2}{(1+\sqrt{2})^2 (1+\mu)^2 \bar{\varepsilon}_x \omega^2}, \tag{75}$$

then, for any fault satisfying $f \in \mathscr{F}_{\min}, \forall t \geq t_f$, with $t_f \geq T_s$ by considering the residual evaluation function (45), the threshold function (71) guarantees the weak isolation of fault f whenever $-\delta \leq \delta_a \leq \delta, \forall t \geq T_s$, where T_s is obtained as

$$T_s = \eta^{-1} \ln \frac{\eta \vartheta}{((1+\mu)^2 - 1) J_{th\infty}^2}, \tag{76}$$

with $J_{th\infty} := \sqrt{\gamma d_{\max}^2 + \alpha_1 \bar{\varepsilon}_x \omega^2}$.

Proof. The proof is directly obtained by the proof of Theorem 4 considering $T_0 = T_s$ in (62), with T_s given in (76). Moreover, when (72) holds, then uncertainties in the range $\delta_a \in [-\delta, \delta]$ and $d_f \in \mathcal{D}_f$ will not trigger the FDI device.

Theorem 5 considers a given α_0 in which false positive alarms cannot occur when the piecewise constant threshold (71) is used, and weak isolation is guaranteed, where the value of $J_{th\infty}$ represents the threshold (51) when $T_s \to \infty$, and the scalar μ represents $(J_{th}(t) - J_{th\infty})/J_{th\infty}$. However, a fault might not be detected at some instants during the interval $t < T_s$ if α_0 is not properly chosen, which will lead to a detection delay. Moreover, although smaller values of μ can reduce conservativeness, time T_s can increase, which means that a fault can remain undetected for a longer period, with the maximum detection delay given by:

$$t_d := T_s - T_{\min}, \ T_s \geq T_{\min} \geq t_f,$$

where $T_{\min}$ is the time in which $\|f\| = f_{\min}$ for the first time[4]. Algorithm 1 provides a method to obtain the parameters for (71) such that strong isolation may be guaranteed during the time interval $t \in [0, T_s)$ whenever $\|f\| \geq f_{0\min}$, where $f_{0\min}$ must be obtained, and weak isolation can be guaranteed for the given $f_{\min}$, such that a fault with magnitude $f_{\min}$ is guaranteed to be detected after time T_s.

Algorithm 1 Obtaining the threshold function

Input: $\eta > 1$, ω^2 satisfying (16), $\mu \in (0, 1]$, $f_{\min}$ satisfying (48) and $e(0) \in \Omega_0$
Input: Matrices P, H_i, L_i, and scalars $\beta, \varepsilon_{xi}, \gamma, \vartheta$ obtained as a solution to the optimization problem (43)–(44) in Theorem 3 $\forall i \in \mathbb{I}_{\mathscr{M}}$ considering η and ω.

```
if optimization (61)–(63) in Theorem 4 has solution ∀i ∈ I_M and δ = 1 then
    J_th(t) is defined as in (51) for all t ≥ 0, with T_0 = 0
else
    if optimization (68)–(70) in Corollary 1 has solution ∀i ∈ I_M then
        α_0 ← α
    else
        α_0 ← 1
    end
    if optimization (73)–(75) in Theorem 5 has solution ∀i ∈ I_M then
        T_s ← T_s, δ ← δ, J_th(t) is defined as in (71), for all t ≥ 0.
    else
        J_th(t) is defined as in (51), for all t ≥ 0, with α = 1 and T_s = 0, δ ← −0.15.
    end
end
```

If $\delta = 1$ is obtained applying Algorithm 1, then a piecewise constant threshold does not need to be considered, since strong isolation is guaranteed with $J_{th}(t)$ in (51). On the other hand, strong isolation may be guaranteed only for some $f_{0\min} > f_{\min}$, or even the optimization problem in Corollary 1 has no solution. In the former scenario, there is no guarantee that a fault is detected if $f_{\min} \leq \|f\| < f_{0\min}$ for some $t \in [t_f, T_s)$. Still, if $\|f\| \geq f_{0\min}, \forall t \in [t_f, T_s)$ strong isolation is still ensured during this interval, whereas if the optimization in Theorem 5 has a solution, then weak isolation is guaranteed if $\|f\| \geq f_{\min}, \forall t \geq T_s$ for $\delta_a \in [-\delta, \delta]$ and $d_f \in \mathcal{D}_f$. However, if it is not possible to find a threshold (51) or the piecewise constant threshold (71) that guarantees weak isolation for the given $f_{\min}$ considering parameters β, η_f, γ, ε_{xi} and ω as well as the matrices P, M_i, N_i for all $i \in \mathbb{I}_{\mathscr{M}}$, then a different $f_{\min}$ must be considered. In this scenario, Algorithm 1 will have a default value of $\delta \notin [0, 1]$ as the output, defined in this work as -0.15.

[4] The instant $T_{\min}$ has a different meaning from T_D, since the latter considers the detection time and $T_{\min}$ is the first time in which $\|f\| \geq f_{\min}$, which may not be equal due to detection delay t_d, although $\|f(T_{\min})\| = \|f(T_D)\| = f_{\min}$. On the other hand, when $T_s = 0$, we have $T_{\min} = T_D$.

Remark 4. In a simultaneous faults scenario, the times of occurrence of faults are the same, i.e., $t_f^\ell = t_f^m, \forall\{\ell, m \in \mathbb{F} : m \neq \ell\}$, but the detection of each fault $f^\ell \in \mathscr{F}$ does not necessarily occur at the same time, even when fault isolation is guaranteed. In fact, when fault isolation of all faults $f^\ell \in \mathscr{F}$ is achieved, but the detection times are different, i.e., $T_D^\ell \neq T_D^m, \forall \ell, m \in \mathbb{F}$ then $a^\ell(t) = 1$ for all $t \geq T_D^\ell$, and $a^m(t) = 1$, for all $t \geq T_D^m$, whereas $a^\ell(t) = 0$ for all $t < T_D^\ell$, and $a^m(t) = 0$, for all $t < T_D^m$. Also, if $T_D^\ell > T_D^m$, then $\alpha^\ell(t) = 0$ for all $t \in [0, T_D^m] \bigcup [T_D^m, T_D^\ell)$, whereas $\alpha^m(t) = 0$ only for $t \leq T_D^m$. Still, weak and strong isolation guarantees the detection and isolation of fault f^ℓ in finite time even if all remaining sensor are faulty (multiple faults), i.e., $\|f^m\| > 0, \forall m \in \mathbb{F}, \forall m \neq \ell, \forall t \geq T_D^\ell$, and for all $\delta_a \in [-1, 1]$ (strong isolation) or $\delta_a \in [-\delta, \delta]$ (weak isolation). Moreover, the results presented in this remark can be extended for any sequence of sensor faults since the time of the occurrence of the remaining fault does not affect the time of the detection of fault f^ℓ.

By solving the optimization problem in Theorem 3, the gains L_i^ℓ, R_i^ℓ for all $i \in \mathbb{I}_\mathscr{M}$ and $\ell \in \mathbb{F}$ are obtained to guarantee $\mathcal{S}_-$ and $\mathcal{L}_\infty$ performances, and by Theorem 4 we provide the maximum range of the uncertainty and a threshold function in which weak isolation and a mixed $\mathcal{S}_-/\mathcal{L}_\infty$ performance are guaranteed. Moreover, by applying Algorithm 1 it is possible to obtain a piecewise constant threshold to reduce the conservativeness in the FDI problem. However, the parameter η affects the solutions of Theorem 3 and, by consequence, the threshold function and δ obtained in Algorithm 1 may vary as different values of η in Theorem 3 are adopted.

In the following section, we propose a parameter tuning algorithm to find a local optimum value for η to obtain the local maximum range of δ_a in which weak isolation is still guaranteed when the residual evaluation and threshold functions (45), and (51) are considered. From now on, the index ℓ to represent each observer will be considered again. The results obtained so far for one residual error generator and threshold functions still hold for all $\ell \in \mathbb{F}$ without loss of generality.

4.3. Parameter tuning algorithm

Let $\eta_{\max}$ be a chosen maximum value of η^ℓ to satisfy (22), (21) and (33) in Theorem 3, such that

$$1 < \eta_{\max} < -2\overline{\lambda}_{\max}(A_i + \delta_a Q_i), \forall i \in \mathbb{I}_\mathscr{M}, \ell \in \mathbb{F},$$

where $A_\sigma + \delta_a Q_\sigma$ are Hurwitz for any $\sigma = i, \forall i \in \mathbb{I}_\mathscr{M}$ and any δ_a satisfying (4). Also, let η_{steps} be the interval between all values in a vector $\mathbf{n} \in \mathbb{R}^{\tilde{k}_{\max}}$, such that $\mathbf{n}(1) = 1 + \eta_{\text{steps}}$, $\mathbf{n}(k_{\max}) = \eta_{\max}$ and $\eta_{\text{steps}} = \mathbf{n}(\tilde{k}+1) - \mathbf{n}(\tilde{k})$, with $\tilde{k} \in \tilde{K}_\eta$ an integer index, where $\tilde{K}_\eta := \{1, \ldots, \tilde{k}_{\max}\}$, and let $f_{\min}^\ell \leq f_{\max}^\ell, \forall \ell \in \mathbb{F}$ be given and vectors $\mathcal{V}^\ell(\tilde{k})$ be composed by the solutions proposed in the algorithm for all $\tilde{k} \in \tilde{K}_\eta$ for each $\eta^\ell \in \mathbf{n}$ and $\ell \in \mathbb{F}$, respectively. In what follows, Algorithm 2 provides the maximum range of uncertainties $\delta_a \in [-\delta_*, \delta_*]$ in which weak or strong isolation of fault f^ℓ is achieved, where $0 \leq \delta_* \leq 1$ is the optimization variable to be found. Parameters δ^ℓ and δ_*^ℓ for each $\ell \in \mathbb{F}$ represent a range and maximum range of uncertainties, respectively, in which weak (or strong) isolation of the ℓ^{th} fault is still guaranteed for the given $f_{\min}^\ell$.

Algorithm 2 aims to find the values of η in which the solution of the optimization problem in Theorem 3 and Algorithm 1 maximizes the range of δ_a in which weak isolation of a fault f^ℓ is guaranteed with respect to $f_{\min}$, obtained as $\delta_a \in [-\delta_*, \delta_*]$. If $\delta_*^\ell = -0.10$, there is no η that satisfies the optimization problem in Theorem 3, which is possible if the values of $\omega^2, f_{\max}^\ell$ and $d_{\max}^\ell$ are very high or if the matrices A_i, b_i or C_i are ill-conditioned. In this scenario, the designer should consider a switching strategy to reduce ω^2, or smaller fault bounds $f_{\max}^\ell$ and $d_{\max}^\ell$, or even a time-scaling in system (5) as the one applied in Carneiro et al. (2024). On the other hand, $\delta_*^\ell = -0.15$ means that there is no threshold obtained by Algorithm 1 that guarantees weak isolation for a given $f_{\min}^\ell$.

Algorithm 2 Tuning of parameters η^ℓ

Input: ω satisfying (16), $\mu \in (0, 1]$, $f_{\min}$ satisfying (48) and $e(0) \in \Omega_0$

```
for ℓ = 1, ⋯ , p do
    for k̃ = 1, ⋯ , k̃_max do
        η^ℓ ← n(k̃)
        if optimization (43)–(44) in Theorem 3 has solution ∀i ∈ I_M then
            Run Algorithm 1
            V^ℓ(k̃) ← δ^ℓ
        else
            V^ℓ(k̃) ← −0.10
        end
    end for
    k̃*^ℓ ← min_{k̃∈K̃η} ( arg max_{k̃∈K̃η} (V^ℓ(k̃)) ),  η*^ℓ ← n(k̃*^ℓ)
end for
δ* ← min_{ℓ∈F} V^ℓ(k̃*^ℓ)
```

Furthermore, in the best-case scenario of the solution of Algorithm 2, the parameter δ_* obtained is equal to one, and strong isolation is guaranteed. On the other hand, if it is still possible to find a solution for the optimization problems in Theorem 3 and Algorithm 1, the worst-case scenario obtained by Algorithm 2 is $\delta_* = \alpha^\ell(\tilde{k}_*^\ell) = 0, \forall \ell \in \mathbb{F}$, which implies that weak isolation is achieved only if system (3) is a switched affine system without uncertainties. Furthermore, observer gains L_i^ℓ, R_i^ℓ, parameters γ^ℓ, $\overline{\varepsilon}_x^\ell$, β^ℓ, α^ℓ and the threshold functions as in (51) or in (71) for all $i \in \mathbb{I}_\mathscr{M}$ and $\ell \in \mathbb{F}$ are obtained by selecting $\eta = \eta_*^\ell$ in Theorem 3 and by applying Algorithm 1.

5. Numerical example

Consider a bidirectional DC–DC Cuk converter with parasitic resistances as in Bashir, Jamil, Yamin, and Ullah (2021), where the switching position is defined as system modes, such that $\sigma = i = 1$ and $\sigma = i = 0$ corresponds to the on and off state of the active switching device, respectively. Also, we considering a value of the load resistance, varying 10% around the nominal value R_o such that the uncertain load resistance is given by $R_o \pm \overline{R_o}$, where $\overline{R_o}$ is the maximum variation given by $\overline{R_o} := 0.1R_o$. The dynamics of the converter are thus written as an uncertain SAS (3), with $x(t) = [i_{L1}, v_{C1}, i_{L2}, v_{C2}]'$, $b_1 = b_2 = [V_{in}/L_{in1}, 0, 0, 0]'$, $F_1 = F_2 = I_3$ and with the following matrices

$$A_1 = \begin{bmatrix} -\frac{R_{L1}+R_s}{L_{in1}} & 0 & 0 & 0 \\ 0 & 0 & \frac{-1}{C_{o1}} & 0 \\ -\frac{R_s}{L_{in2}} & \frac{1}{L_{in2}} & a_1^{33} & a_1^{34} \\ 0 & 0 & \frac{R_o}{C_{o2}(R_o+R_{C2})} & a_1^{44} \end{bmatrix},$$

$$A_2 = \begin{bmatrix} -\frac{R_{C1}+R_{L1}+R_D}{L_{in1}} & -\frac{1}{L_{in1}} & -\frac{R_D}{L_{in1}} & 0 \\ \frac{1}{C_{o1}} & 0 & 0 & 0 \\ -\frac{R_D}{L_{in2}} & 0 & a_2^{33} & a_1^{34} \\ 0 & 0 & \frac{R_o}{C_{o2}(R_o+R_{C2})} & a_1^{44} \end{bmatrix},$$

$$a_1^{33} = -\frac{R_s + R_{C1} + R_{L2}}{L_{in2}} - \frac{R_o R_{C2}}{L_{in2}(R_o + R_{C2})},$$

Table 1
Parameters of the Cuk converter.

Parameter	Value	Description
L_{in1}	1 mH	Inductance of inductor 1
L_{in2}	2 mH	Inductance of inductor 2
C_{o1}	100 µF	Capacitance of capacitor 1
C_{o2}	2 mF	Capacitance of capacitor 2
R_{L1}	0.1 Ω	Parasitic resistance of inductor 1
R_{L2}	0.2 Ω	Parasitic resistance of inductor 2
R_{C1}	10 mΩ	Parasitic resistance of capacitor 1
R_{C2}	10 mΩ	Parasitic resistance of capacitor 2
R_S	0.10 mΩ	Switch resistance
R_D	0.01 mΩ	Diode resistance
R_o	3 Ω	Nominal Load resistance
$\overline{R_o}$	0.3 Ω	Maximum variation of Load resistance
V_{in}	25 V	Input source voltage (constant)

$$a_1^{34} = -\frac{R_o}{L_{in2}(R_o + R_{C2})},\ a_1^{44} = -\frac{1}{C_{o2}(R_o + R_{C2})},$$

$$a_2^{33} = -\frac{R_{L2} + R_D}{L_{in2}} - \frac{R_o R_{C2}}{L_{in2}(R_o + R_{C2})},$$

$$C_1 = C_2 = \begin{bmatrix} 0 & 0 & \frac{R_{C2}R_o}{R_{C2}+R_o} & \frac{R_o}{R_{C2}+R_o} \\ 1 & 0 & 0 & 0 \\ 0 & 0 & 1 & 0 \end{bmatrix},$$

and $Q_1 = M_1 N_1,\ Q_2 = M_2 N_2$ with

$$M_1 = M_2 = \begin{bmatrix} 0 & 0 & 0 & 0 \\ 0 & 0 & 0 & 0 \\ q_1^{33} & q_1^{34} & 0 & 0 \\ q_1^{43} & q_1^{44} & 0 & 0 \end{bmatrix},\ N_1 = \begin{bmatrix} 0 & 0 & 1 & 0 \\ 0 & 0 & 0 & 1 \\ 0 & 0 & 0 & 0 \\ 0 & 0 & 0 & 0 \end{bmatrix}$$

$$q_1^{33} = \frac{R_o R_{C2}}{L_{in2}(R_o + R_{C2})} - \frac{(R_o + \overline{R_o})R_{C2}}{L_{in2}((R_o + \overline{R_o}) + R_{C2})}$$

$$q_1^{34} = \frac{R_o}{L_{in2}(R_o + R_{C2})} - \frac{R_o + \overline{R_o}}{L_{in2}((R_o + \overline{R_o}) + R_{C2})}$$

$$q_1^{43} = -\frac{R_o}{C_{o2}(R_o + R_{C2})} + \frac{R_o + \overline{R_o}}{C_{o2}((R_o + \overline{R_o}) + R_{C2})}$$

$$q_1^{44} = \frac{1}{(R_o + R_{C2})C_{o2}} - \frac{1}{((R_o + \overline{R_o}) + R_{C2})C_{o2}}$$

where $\Delta\overline{R_o}$ is a function of $\delta_a(t)$ that satisfies

$$\Delta\overline{R_o}(\delta_a(t)) = -R_o + \frac{Ro(Ro + \overline{R_o})}{Ro + (1 - \delta_a(t))\overline{R_o} + R_{C2}} + \frac{R_{C2}(R_o + \delta_a(t)\overline{R_o})}{Ro + (1 - \delta_a(t))\overline{R_o} + R_{C2}}.$$

and $i_{L1},\ i_{L2}$ are inductor currents, $v_{C1},\ v_{C2}$ are capacitor voltages. The value and description of all variables in matrices A_i and b_i for all $i \in \mathbb{I}_{\mathscr{M}}$ are in Table 1.

Without sensor faults, the output of the uncertain system is $y = C_1 x$, hence $y = [v_o, i_{L1}, i_{L2}]'$, where $v_o = (R_{C2}R_o)/(R_{C2} + R_o)i_{L2} + R_o/(R_{C2}+R_o)v_{c2}$ is the output voltage, and each sensor represents each state variable, such that the ℓ^{th} sensor corresponds to the sensor in the position ℓ of y. For instance, $\ell \in \mathbb{F} = 3$ corresponds to the measurements of the sensor for the second inductor current i_{L2}. An schematic of FDI scheme applied to the Cuk converter is represented in Fig. 1.

Moreover, $\omega^2 = \max_{t\in[0,T_f]} \|N_1 x(t)\|^2 = \max_{t\in[0,T_f]} \|N_2 x(t)\|^2$ is obtained considering the following Pulse-Width Modulation (PWM)-type switching signal:

$$\sigma(t) = 2 - 0.5\text{sign}(\sin 2\pi 20\,\text{k}t), \tag{77}$$

corresponding to a duty cycle of 50% and switching frequency of 20 kHz applied in the DC–DC converter, with an initial condition of $x(0) = [1.424, 9.416, 1.424, 4.274]'$ in the set Ω_0 defined in Assumption 3, with $\|x(0)\|^2 = 110.259 < \omega_0^2$, $\omega_0^2 = 625$, corresponding to a previous operation point before applying the FDI Devices and $T_f = 0.6$ s is the final time of the simulation.

Moreover, we considered a known square-wave uncertainty function defined as follows:

$$\delta_a(t) = -\delta\ \text{sign}(\sin 2\pi f_\delta t), \forall t \in [0, T_f]. \tag{78}$$

where $f_\delta = 20$ Hz, which corresponds to a variation with slow development comparing to the PWM frequency, in order to avoid parametric resonance.

Although it is not possible to estimate ω precisely, we considered $\omega^2 = \max_{t\in[0,T_f]} \|N_1 x(t)\|^2$, which was obtained for the given initial condition, switching signal, and uncertainty function (78), considering 100 simulations applying different variant values of δ varying from -1 to 1 with an increment of 0.0202. The maximum value of ω were then obtained for $\delta = 1$, which corresponds to a load increase of 0.30 Ω resulting in $\omega^2 = 823.977$. The values of $\|N_1 x(t)\|^2$ during the time interval $t \in [0, T_f]$ for $\delta = 1$ are shown in Fig. 2 along with the switching signal and uncertainty function and ω. The trajectories of the switched system and output voltages are shown in Fig. 3.

To verify the application of the proposed pseudo-dedicated observer scheme, suppose that classical DOS or GOS using residual error generators composed by Luenberger observers are considered to detect and isolate faults in all sensors in the proposed Cuk DC–DC converter. To detect and isolate faults in all 3 sensors, the classical GOS requires a number of 3 observers with order $3-1 = 2$ (i.e., at least one sensor is not considered in the observer design for robust isolation), whereas the classical DOS requires 3 observers with order 1 (for full isolation). To exemplify the use of a classical GOS in the proposed Cuk DC–DC converter, consider a set $\mathcal{S} := \{\mathcal{S}^1, \mathcal{S}^2, \mathcal{S}^3\}$ such that each subset $\mathcal{S}^\ell$ of $\mathcal{S}$ represents a set of all 3 sensor indices except the ℓ^{th} index, considered for each observer design. To design one of the observers to detect faults in sensor 2, i.e, using set $\mathcal{S}^2$, use a matrix C^- corresponding to the matrix C_1 removing the second row and y^- the output vector excluding the second element. In the scenario in which the measurement of the second sensor is not considered, both GOS and DOS will not be able to provide FDI of faults in sensor 2, making the observer design infeasible since the pair (A_2, C^-) is not observable. Additionally, since observability is not guaranteed using sensors 1 and 3 simultaneously, thus it is not possible to guarantee observability using only sensor 1 or sensor 3 to design observers following the DOS structure. On the other hand, the proposed pseudo-dedicated observer scheme considers that the measurements of all sensors can be used in the FDI strategy. Thus, considering a set of 3 observers using the information of all 3 sensors, it is possible to verify that all pairs (A_i, C_i) for all $\sigma = i, \forall i \in \mathbb{I}_{\mathscr{M}}$, are observable, which satisfies Assumption 2. Therefore, the pseudo-dedicated observer scheme proposed is adequate for the detection and isolation of faults in all sensor.

Considering ω obtained previously, the next section presents the design of the FDI devices for all $f^\ell \in \mathscr{F}$ sensor faults and simulation results.

5.1. Design of the FDI devices

Considering the representation in (5), vector f_s can be written as $f_s = \left[f^1, f^2, f^3\right]'$. Also, it is straightforward to verify that

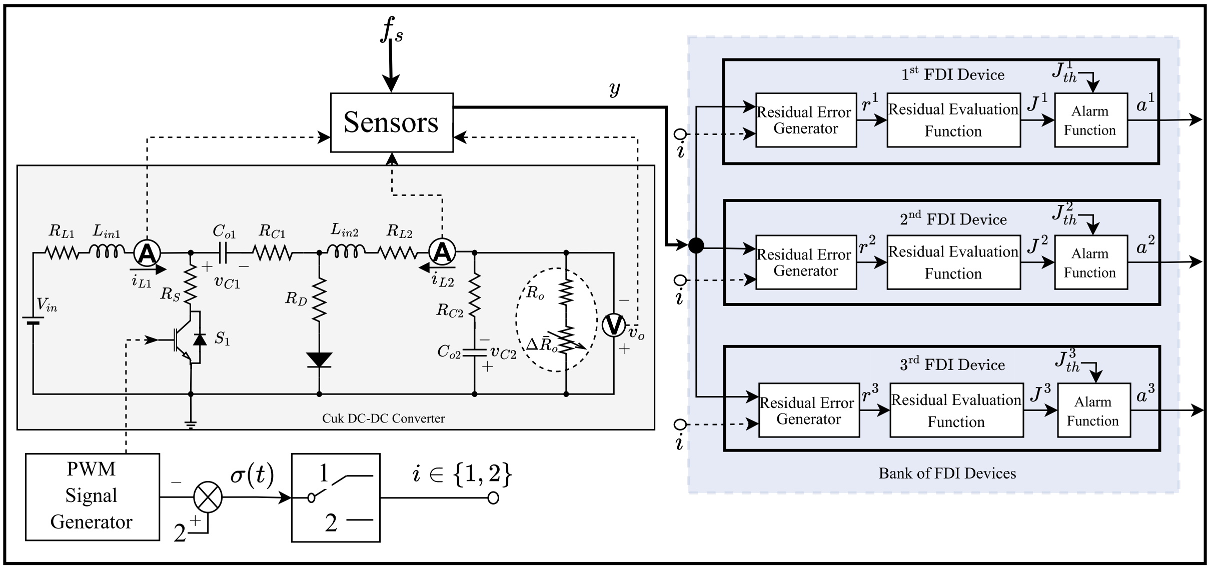

Fig. 1. FDI scheme of the Cuk converter with parasitic resistances. The thresholds J^{ℓ}_{th} corresponds to threshold functions (51) or (71) and a^{ℓ} is the alarm function as defined in (17), for each $\ell \in \mathbb{F}$.

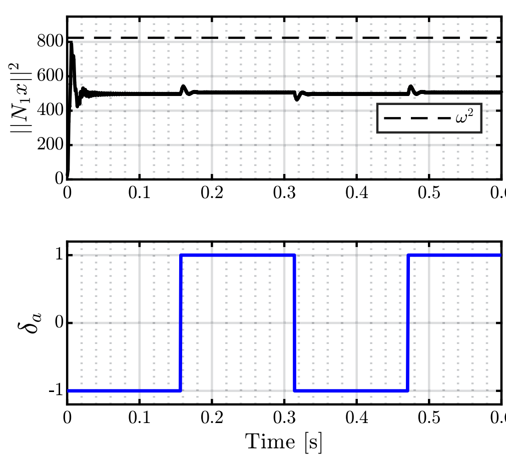

Fig. 2. The bound ω^2 as in (16) applying PWM-type switching signal (77) in (5) without faults. The uncertainty function is represented in blue, with $\delta = 1$ and uncertainty function (78).

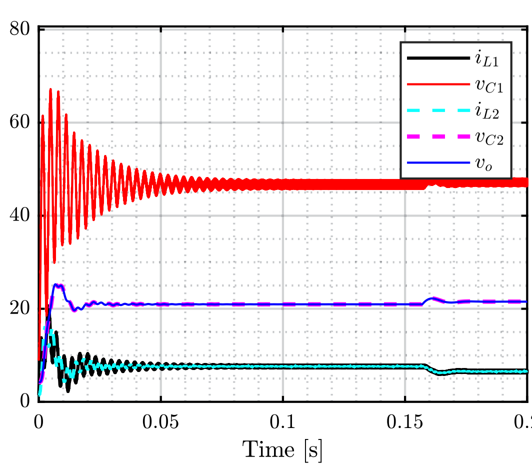

Fig. 3. Trajectories of the switched system and output voltage during the transient phase, where $\|x\|$ reaches its maximum.

Table 2
Bounds of sensor faults.

ℓ	$f^{\ell}_{\max}$	$d^{\ell}_{\max}$	$f^{\ell}_{\min}$
1	106.232	50.078	16.997
2	35.411	111.979	5.667
3	35.411	111.979	5.667

$d^1_f = [f^2, f^3]'$, $d^2_f = [f^1, f^3]'$ and $d^3_f = [f^1, f^2]'$. Then, the maximum magnitude of all sensor faults and remaining faults can be determined individually for each $i \in \mathbb{I}_{\mathscr{M}}$. Moreover, the smallest fault magnitude to be detected for each sensor was given as $f^{\ell}_{\min} = 0.16 f^{\ell}_{\max}$, $\forall \ell \in \mathbb{F}$. The values considered for $f^{\ell}_{\max}$, $d^{\ell}_{\max}$ and $f^{\ell}_{\min}$ are present in Table 2, where values of $d^{\ell}_{\max}$, $\forall i \in \mathbb{I}_{\mathscr{M}}$ are obtained by adding the contribution of the magnitude of all faults except the faults in the ℓth sensor and the maximum magnitude $\bar{f}_{\max}$ for f_s is obtained as $\bar{f}_{\max} = \sqrt{\sum_{\ell \in \mathbb{F}} {f^{\ell}_{\max}}^2} = 117.44$.

The design of the bank of residual error generators and threshold functions for all FDI devices are obtained simultaneously by applying Algorithm 2. The initial conditions of all observers were defined as $z^{\ell}(0) = [1.416, 0, 1.416, 4.249]$, considering Proposition 1, such that $\|e_z(0)\|^2 = 88.19 < \omega_0^2$. The value of δ_* was obtained considering $\mu = 0.05$, $\eta_{\max} = 60$, $\eta_{\text{steps}} = 1$, $\omega^2 = 823.977$, $\omega_0^2 = 625$, $k_{\max} = 59$, and considering the parameters $f^{\ell}_{\max}$, $d^{\ell}_{\max}$ and $f^{\ell}_{\min}$ obtained in Table 2, resulting in $\delta_* = 0.188$. Also, Fig. 4 shows the variation of δ^{ℓ} as η changed for each FDI Device. The remaining parameters obtained after applying Algorithm 2 are given in Table 3, and Table 4. Observe that was possible to find smallest fault magnitudes to be detected that satisfies strong isolation conditions for any $t \geq 0$ for FDI Devices 1. On the other hand, it is not possible to achieve strong isolation condition using FDI Device 2 and 3, i.e., there no exists $f^2_{\min} \leq f^2_{\max}$ and $f^3_{\min} \leq f^3_{\max}$ such that strong isolation is guaranteed for any $t \geq 0$.

Considering $\eta^{\ell} = \eta^{\ell}_*$ in Theorem 3 for all $i \in \mathbb{I}_{\mathscr{M}}$, $\ell \in \mathbb{F}$, we obtain the residual error generator gain matrices L^{ℓ}_i, R^{ℓ}_i for all $i \in \mathbb{I}_{\mathscr{M}}$, $\ell \in \mathbb{F}$. However, the resulting matrices P^{ℓ}, H^{ℓ}_i, W^{ℓ}_i, L^{ℓ}_i, R^{ℓ}_i, are not presented in this manuscript due to space limitations. Still, all data are available in a Mendeley repository at Carneiro, Faria, Oliveira, Cucuzzella, and Ferrara (2025).

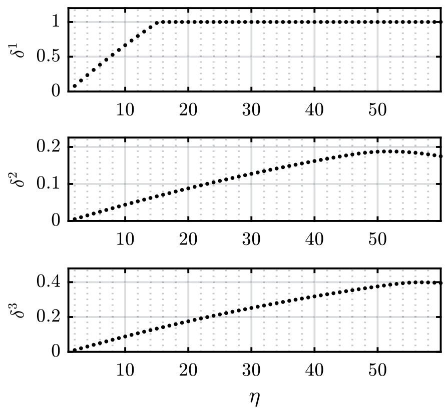

Fig. 4. The first plot (from top to bottom) represents the evolution of δ^1 according to η using Algorithm 2. The second and third plots are related to the evolution of δ^2 and δ^3, respectively.

Table 3
Optimization parameters obtained after applying Algorithm 2.

ℓ	$\tilde{k}_*^\ell$	η^ℓ	$\eta_f^\ell \times 10^5$	β^ℓ	δ_*^ℓ	$f_{0\,\min}^\ell$
1	16	17	8.639	0.416	1	31.704
2	51	52	8.030	1.955	0.188	∄
3	56	57	10.312	4.547	0.399	∄

Table 4
Parameters obtained for all threshold functions.

ℓ	$\gamma^\ell \times 10^{-8}$	$\bar{\varepsilon}_x^\ell$	ϑ^ℓ	α_0^ℓ	α_1^ℓ	T_s^ℓ
1	2.0891	0.0206	18.753	1	1	0.3064
2	2.508	0.0631	50.512	1	0.188	0.1514
3	4.822	0.0692	54.412	1	0.399	0.1262

The values of δ_*^ℓ are small since the method to obtain these values is conservative, and the $f_{\min}^\ell$ values considered are not sufficiently high to guarantee strong isolation for all faults. However, with $f_{\min}^1 = 16.997$ it is possible to ensure strong isolation of faults in the sensor 1 (output voltage sensor). In the next section, we are going to show through simulation results that weak isolation for all sensor faults is obtained considering the uncertainty function (78) with $\delta = \delta_* = 0.1888$.

5.2. Simulation of sensor faults

To illustrate the effectiveness of the proposed approach, we considered permanent abrupt sensor faults as in Definition 2. These faults were modeled as offset faults, characterized by a constant magnitude ϕ^ℓ after the time of the fault occurrence t_f^ℓ, in which the magnitude and the time of occurrence of each fault depend on each simulation scenario, according to Table 5. The simulations for each scenario are presented in Figs. 5(a), 5(b), 5(c), 5(d), 5(e) and 5(f), respectively, considering a residual evaluation function as in (45) with $T = 10^{-3}$ s and piecewise constant threshold functions with parameters given in Table 2 and 4. The scenarios 1 to 3 represent simultaneous faults occurring before switching time T_s^ℓ for each $\ell \in \mathbb{F}$, whereas scenarios 4 to 6 consist in consecutive faults in which a fault in sensor ℓ occurs before T_s^ℓ.

The simulation results show that for an uncertainty function with $\delta = \delta_* = 0.188$, the FDI devices guarantee weak isolation of simultaneous and consecutive faults whenever the smallest fault magnitude to be detected in each $\ell \in \mathbb{F}$ sensor is greater than or equal $f_{\min}^\ell$. Observe that in all scenarios, $a^\ell = 1$ only after the occurrence of the corresponding ℓ^{th} sensor fault, which

Table 5
Parameters obtained for all FDI devices.

Scenario	δ	ϕ_2^1	ϕ_2^2	ϕ_2^3	t_f^2	t_f^2	t_f^3
1	0.188	$f_{\min}^2$	$f_{\max}^2$	$f_{\max}^3$	$2T_s^1$	$2T_s^1$	$2T_s^1$
2	0.188	$f_{\max}^2$	$f_{\min}^2$	$f_{\max}^3$	$2T_s^2$	$2T_s^2$	$2T_s^2$
3	0.188	$f_{\max}^2$	$f_{\max}^2$	$f_{\min}^3$	$2T_s^3$	$2T_s^3$	$2T_s^3$
4	0.188	$f_{\min}^2$	$f_{\max}^2$	$f_{\max}^3$	$0.75T_s^1$	$0.25T_s^1$	$0.25T_s^1$
5	0.188	$f_{\max}^2$	$f_{\min}^2$	$f_{\max}^3$	$0.25T_s^2$	$0.75T_s^2$	$0.25T_s^2$
6	0.188	$f_{\max}^2$	$f_{\max}^2$	$f_{\min}^3$	$0.25T_s^3$	$0.25T_s^3$	$0.75T_s^3$

shows that weak isolation is achieved for FDI Devices 2 and 3, whereas strong isolation is achieved in sensor 1 with given $f_{\min}^1$. However, weak and strong isolation are achieved after a time $t \geq T_s^\ell \geq t_f^\ell$, for each fault f^ℓ, $\forall \ell \in \mathbb{F}$, which means that, although uncertainties and remaining faults cannot trigger the FDI Devices, a detection delay is present whenever $t_f^\ell < T_s^\ell$, $\forall \ell \in \mathbb{F}$.

6. Conclusions

We provided a robust solution to detect and isolate simultaneous and consecutive permanent abrupt sensor faults in a class of uncertain SAS that combines $\mathcal{S}_-$ and $\mathcal{L}_\infty$ fault sensitivity and attenuation performances, respectively, along with optimal threshold functions for a range of uncertainties and the smallest fault to be detected. The optimization problem proposed in Theorem 3 provides the residual error generators gains to enhance sensitivity to specific faults while attenuating the effect of uncertainties and remaining faults in the residual.

Moreover, Theorem 4 provides a threshold value that guarantees weak isolation for faults with magnitudes exceeding a given value for the maximum range of uncertainties functions, whereas Corollary 1 provides sufficient conditions and a value for the smallest fault magnitude to be detected to guarantee strong isolation. Furthermore, Theorem 5 provides an LMI-based optimization problem to obtain less conservative conditions to achieve weak isolation when the initial estimation error is nonzero. Finally, Algorithms 1 and 2 provide the gains and threshold functions so that the weak isolation is guaranteed for a maximum range of uncertainties according to the value associated with the decay rate.

The numerical example has shown that the method of threshold calculation by choosing parameters α_0^ℓ and α_1^ℓ for each $\ell \in \mathbb{F}$ provides a degree of freedom in the threshold design based on the attenuation gains obtained via LMIs, which can be useful for practical applications.

Acknowledgments

This research is a collaboration between the Control Laboratory in the Electrical Engineering Department of Escola de Engenharia de São Carlos, Universidade de São Paulo, and the Intelligent Robotics Laboratory at the University of Pavia. This work was supported by the Brazilian National Research Council (CNPq) under grant 311959/2021-0, by the Research Development Foundation (FUNDEP), Brazil Rota 2030/Line V under grant 27192/27, and by The São Paulo Research Foundation (FAPESP) under grants 2014/50851-0, 2019/25530-9, and 2022/01074-7. It is also partially supported by Project E-COSMOS under grant BIITASRB24_00069.

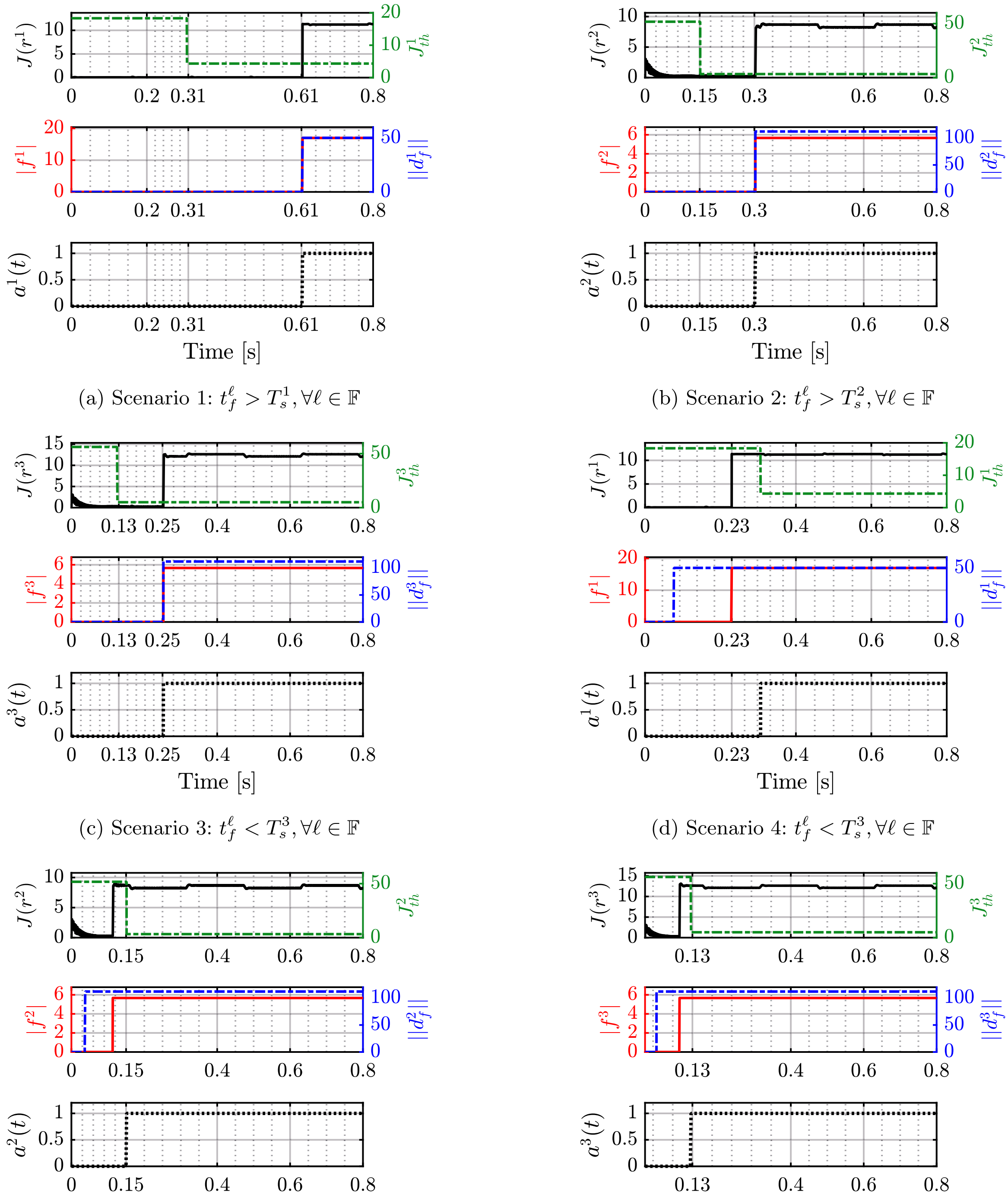

(a) Scenario 1: $t^\ell_f > T^1_s, \forall \ell \in \mathbb{F}$

(b) Scenario 2: $t^\ell_f > T^2_s, \forall \ell \in \mathbb{F}$

(c) Scenario 3: $t^\ell_f < T^3_s, \forall \ell \in \mathbb{F}$

(d) Scenario 4: $t^\ell_f < T^3_s, \forall \ell \in \mathbb{F}$

(e) Scenario 5: $t^\ell_f < T^3_s, \forall \ell \in \mathbb{F}$

(f) Scenario 6: $t^\ell_f > T^3_s, \forall \ell \in \mathbb{F}$

Fig. 5. For all simulated scenarios, the black solid lines in the first axis correspond to the residual evaluation function, whereas the dashed green lines corresponds to the threshold functions; the red solid lines and dashed blue lines correspond to the absolute value of the fault in sensor ℓ ($|f^\ell|$) and magnitude of remaining faults $\|d^\ell_f\|$, respectively; the gray dotted line in the third plot represents the alarm function. For Scenarios 1 to 3, a fault in all sensors occur at $t = 2T^\ell_s$ (simultaneous fault). On the other hand, in Scenarios 4 to 6, the fault in all sensors except sensor ℓ occurs at $t = 0.25T^\ell_s$, and the fault in sensor ℓ occurs at $t = 0.75T^\ell_s$ (consecutive faults). Note that in Scenarios 4 to 6 there is a detection delay $t^\ell_d = T^\ell_s - t^\ell_f$ since the fault occurs before T^ℓ_s. However, the fault is detected for any $t \geq T_s$.

References

Ali, Shafqat, Jiang, Yuchen, Luo, Hao, Raza, Muhammad T., Faisal, Shah, & Shahid, Faizan (2024). Robust fault detection scheme for asynchronous switched systems via sliding mode observer. *International Journal of Control, Automation and Systems*, 1–15.

Alwi, Halim, Edwards, Christopher, & Tan, Chee Pin (2011). Fault detection and fault-tolerant control using sliding modes. In *Advances in industrial control*, (p. 336). London, UK: Springer.

Bashir, Muhammad S, Jamil, Sohaib, Yamin, Zubair, & Ullah, Hameed (2021). Small signal modelling and observer based stability analysis of cuk converter via Lyapunov's direct method. In *2021 international conference on emerging power technologies* (pp. 1–6). IEEE.

Blanke, Mogens, Kinnaert, Michel, Lunze, Jan, & Staroswiecki, Marcel (2016). *Diagnosis and fault-tolerant control*. Berlin, Germany: Springer.

Capisani, Luca M., Ferrara, Antonella, De Loza, Alejandra Ferreira, & Fridman, Leonid M (2012). Manipulator fault diagnosis via higher order sliding-mode observers. *IEEE Transactions on Industrial Electronics*, *59*(10), 3979–3986.

Carneiro, Diego S., Faria, Flavio A., Oliveira, Vilma A., Cucuzzella, Michele, & Ferrara, Antonella (2025). *Data for: Observer-based detection and isolation of bounded permanent sensor faults in a class of uncertain switched affine systems*: *Vol. V1*, Mendeley Data, http://dx.doi.org/10.17632/33rth453ry.1, https://data.mendeley.com/datasets/33rth453ry/1. (Accessed 23 April 2025).

Carneiro, Diego S., Faria, Flávio A., Silva, Lucas J. R., Zilli, Bruno M., & Oliveira, Vilma A. (2024). Robust sampled-observer-based switching law for uncertain switched affine systems subject to sensor faults with an application to a bidirectional buck-boost DC-dc converter. *IEEE Access*, *12*, 87967–87980.

Carneiro, Diego S., Silva, Lucas J. R., Faria, Flávio A., Magossi, Rafael F. Q., & Oliveira, Vilma A. (2021). Reconfiguration strategy for a DC-DC boost converter using sliding mode observers and fault identification with a neural network. In *XV Simpósio Brasileiro de Automação Inteligente* (pp. 1338–1344). http://dx.doi.org/10.20906/sbai.v1i1.2741.

Commault, Christian, Dion, Jean-Michel, Sename, Olivier, & Motyeian, Reza (2002). Observer-based fault detection and isolation for structured systems. *IEEE Transactions on Automatic Control*, *47*(12), 2074–2079.

Du, Dongsheng, Yang, Yue, Zhao, Huanyu, & Tan, Yushun (2020). Robust fault diagnosis observer design for uncertain switched systems. *International Journal of Control, Automation and Systems*, *18*(12), 3159–3166.

Elias, Leandro J., Faria, Flávio A., Araujo, Rayza, Magossi, Rafael F. Q., & Oliveira, Vilma A. (2022). Robust static output feedback $\mathcal{H}_\infty$ control for uncertain Takagi-Sugeno fuzzy systems. *IEEE Transactions on Fuzzy Systems*, *30*(10), 4434–4446.

Gertler, Janos, & McAvoy, Thomas J. (1997). Principal component analysis and parity relations-a strong duality. *IFAC Proceedings Volumes*, *30*(18), 833–838.

Greber, Márton, Fodor, Attila, & Magyar, Attila (2020). Generalized persistent fault detection in distribution systems using network flow theory. *IFAC-PapersOnLine*, *53*(2), 13568–13574.

Hao, Xian-Zhi, & Huang, Jin-Jie (2024). $\mathcal{H}_\infty/\mathcal{H}_-$ filtering fault detection for asynchronous switched discrete-time linear systems with mode-dependent average dwell time. *International Journal of Control, Automation and Systems*, 1–16.

Khargonekar, Pramod R., Petersen, Ian R., & Zhou, Kemin (1990). Robust stabilization of uncertain linear systems: quadratic stabilizability and $\mathcal{H}_\infty$ control theory. *IEEE Transactions on Automatic Control*, *35*(3), 356–361.

Li, Zhuoyu, Ma, Dan, & Zhao, Jun (2021). Dynamic event-triggered $\mathcal{L}_\infty$ control for switched affine systems with sampled-data switching. *Nonlinear Analysis. Hybrid Systems*, *39*, Article 100978.

Marouani, Ghassen, Nguyen, Dang K., Dinh, Thach N., & Raïssi, Tarek (2024). Active fault control based on interval observer for discrete-time linear switched systems. *European Journal of Control*, Article 100991.

Piziak, Robert, & Odell, Patrick L. (1999). Full rank factorization of matrices. *Mathematics Magazine*, *72*(3), 193–201.

Reppa, Vasso, Polycarpou, Marios M., & Panayiotou, Christos G. (2016). Sensor fault diagnosis. *Foundations and Trends® in Systems and Control*, *3*(1–2), 1–248.

Reppa, Vasso, Timotheou, Stelios, Polycarpou, Marios M., & Panayiotou, Christos G. (2017). Optimization of observer design for sensor fault detection of nonlinear systems. In *2017 IEEE 56th annual conference on decision and control* (pp. 5155–5160). IEEE.

Reppa, Vasso, Timotheou, Stelios, Polycarpou, Marios M., & Panayiotou, Christos (2018). Performance index for optimizing sensor fault detection of a class of nonlinear systems. *IFAC-PapersOnLine*, *51*(24), 1387–1394.

Ribeiro, Alexsandra C., Carneiro, Diego S., Costa, Eduardo F., & Oliveira, Vilma A. (2022). Detection of covert attacks on cyber-physical systems using Markovian jump systems. In *XXIV Congresso Brasileiro de Automática* (pp. 1592–1597). http://dx.doi.org/10.20906/CBA2022/3391.

Rinaldi, Gianmario, Cucuzzella, Michele, Menon, Prathyush P., Ferrara, Antonella, & Edwards, Christopher (2022). Load altering attacks detection, reconstruction and mitigation for cyber-security in smart grids with battery energy storage systems. In *2022 European control conference* (pp. 1541–1547). IEEE.

Rinaldi, Gianmario, Menon, Prathyush P., Edwards, Christopher, Ferrara, Antonella, & Shtessel, Yuri B. (2021). Adaptive dual-layer super-twisting sliding mode observers to reconstruct and mitigate disturbances and communication attacks in power networks. *Automatica*, *129*, Article 109656.

Sacchi, Nikolas, Incremona, Gian P., & Ferrara, Antonella (2023). Sliding mode based fault diagnosis with deep reinforcement learning add-ons for intrinsically redundant manipulators. *International Journal of Robust and Nonlinear Control*, *33*(15), 9109–9127.

Su, Qingyu, Fan, Zhongxin, & Li, Jian (2019). $\mathcal{H}_\infty/\mathcal{H}_-$ fault detection for switched systems with all subsystems unstable. *IET Control Theory & Applications*, *13*(12), 1796–1803.

Wheeden, Richard L., & Zygmund, Antoni (1977). Measure and integral: An introduction to real analysis, In *Dekker new york*: *Vol. 26*, (1st ed.). CRC Press.

Xie, Hongzhen, Zong, Guangdeng, Yang, Dong, Chen, Yunjun, & Shi, Kaibo (2022). Dynamic output feedback $\mathcal{L}_\infty$ control of switched affine systems: An event-triggered mechanism. *Nonlinear Analysis. Hybrid Systems*, *47*, Article 101278.

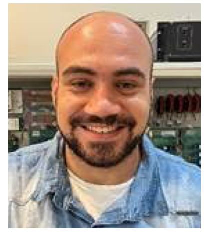

Diego dos Santos Carneiro received his B.Eng. in Control and Automation Engineering from the Federal University of Ouro Preto, Minas Gerais, Brazil, in 2019 and his Ph.D. degree in electrical engineering from the Universidade de São Paulo, Brazil, in 2024. He was a visiting Ph.D. student at the University of Pavia, Pavia, Italy, from May 2022 to February 2023. He is currently a Full R&D Engineer in Guidance, Control and Navigation at XMobots Aerospace & Defense, Brazil. His research interests include fault detection, isolation, and reconfiguration in uncertain switched affine systems.

Flávio Andrade Faria received the B.Math., M.Sc., and Ph.D. degrees in Electrical Engineering from the São Paulo State University (UNESP) in 2003, 2005, and 2009, respectively. Since 2013, he has been an Assistant Professor with UNESP. His research interests include linear-matrix-inequality-based control designs, Takagi–Sugeno fuzzy modeling, and its applications.

Vilma Alves de Oliveira received the B.Eng. degree in electronics from the Universidade do Estado do Rio de Janeiro, Rio de Janeiro, Brazil, in 1976, the M.Sc. degree from the Universidade Federal do Rio de Janeiro, Rio de Janeiro, in 1980, and the Ph.D. degree from the University of Southampton, Southampton, U.K., in 1989, both in electrical engineering. In 1990, she joined the Department of Electrical and Computing Engineering, Universidade de São Paulo, São Paulo, Brazil, where she is currently a Full Professor. Her research interests include fuzzy control and control design and its applications. Prof. Oliveira is currently the Editor in Chief for the Journal of Control, Automation and Electrical Systems.

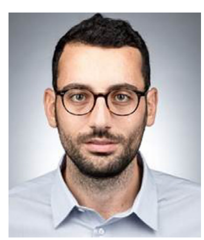

Michele Cucuzzella received the M.Sc. degree in Electrical Engineering and the Ph.D. degree in Systems and Control from the University of Pavia (UP), Italy, in 2014 and 2018, respectively. From 2017 until 2020, he was a postdoc at the University of Groningen (UG), the Netherlands. He then joined the UP as assistant professor and moved in 2024 to the UG as associate professor at the Engineering and Technology institute Groningen. He is also the Twin Transition coordinator at the Jantina Tammes and Wubbo Ockels Schools of the UG and visiting associate professor at the Hiroshima University, Japan. His research activities are mainly in the area of nonlinear control with application to the energy domain and smart complex systems. He has co-authored the book Advanced and Optimization Based Sliding Mode Control: Theory and Applications, SIAM, 2019. He serves as Associate Editor for the European Journal of Control and is member of the EUCA and IEEE CSS Technology Conferences Editorial Boards. He received the Certificate of Outstanding Service as Reviewer of the IEEE Control Systems Letters 2019. He also received the 2020 IEEE Transactions on Control Systems Technology Outstanding Paper Award, the IEEE Italy Section Award for the best Ph.D. thesis on new technological challenges in energy and industry, and the SIDRA Award for the best Ph.D. thesis in the field of systems and control engineering.

Antonella Ferrara received the M.Sc. degree in Electronic Engineering and the Ph.D. degree in Electronic Engineering and Computer Science from the University of Genoa, Italy, in 1987 and 1992, respectively. Since 2005, she has been Full Professor of Automatic Control at the University of Pavia, Italy. Her research activities are mainly in the area of nonlinear control, with a special emphasis on sliding mode control, and application to robotics, power systems and road traffic. She is author and co-author of more than 450 publications including more than 170 journal papers, 2 monographs (published by Springer Nature and SIAM, respectively) and one edited book (IET). She is currently serving as Associate Editor of Automatica, and Senior Editor of the IEEE Open Journal of Intelligent Transportation Systems. She served as Senior Editor of the IEEE Transactions on Intelligent Vehicles, as well as Associate Editor of the IEEE Transactions on Control Systems Technology, IEEE Transactions on Automatic Control, IEEE Control Systems Magazine and International Journal of Robust and Nonlinear Control. Antonella Ferrara is the Chair of the EUCA Conference Editorial Board, the Director of Operations of the IEEE Control Systems Society, the Vice-Chair for Industry of the IFAC TC on Nonlinear Control Systems (2024–2026), and a member of the IFAC Industry Board and IFAC Conference Board. Among several awards, she was a co-recipient of the 2020 IEEE Transactions on Control Systems Technology Outstanding Paper Award. She is a Fellow of IEEE, Fellow of IFAC and Fellow of AAIA. She is also a Senior Fellow of the Brussels Institute for Advanced Studies (BrIAS).